# An Examination of Plasma Membrane Calcium ATPase 2 in the Medial Nucleus of the Trapezoid Body Reveals a Cell Size Gradient

Jessica H. Weatherstone

A dissertation

submitted in partial fulfillment of the

requirements for the degree of

Doctor of Philosophy

University of Washington

2014

Reading Committee:

Bruce Tempel L Chair

Edwin W Rubel

Sandra Bajjalieh

Program Authorized to Offer Degree:

Pharmacology

University of Washington

## Abstract

An examination of PMCA2 localization in the MNTB reveals a cell size gradient

Jessica H. Weatherstone

Chair of Supervisory Committee:

Professor Bruce L Tempel

Otolaryngology-Head and Neck Surgery, Pharmacology

The plasma membrane calcium ATPase 2 (PMCA2) pumps calcium from the cytoplasm to the extracellular space. We show PMCA2 is highly expressed in the medial nucleus of the trapezoid body (MNTB).

*dfw*$^{2J}$ mutant mice have a null mutation in the gene that codes for PMCA2 causing deafness in homozygotes. Because MNTB neurons highly express PMCA2, we postulated that MNTB neurons lacking PMCA2 may have abnormal morphology. We found no significant difference in the gross morphology of MNTBs from *dfw*$^{2J}$ mutants, but did find a decrease in cell size between wildtype and *dfw*$^{2J}$/*dfw*$^{2J}$ mutants.

The MNTB exhibits a tonotopic gradient with medial cells responding best to high frequencies and lateral cells responding best to low frequencies. In wildtype, the medial cells

were significantly smaller than the lateral cells suggesting the presence of a cell size gradient. This size gradient was absent in $dfw^{2J}/dfw^{2J}$.

To determine if the absence of the neuronal size gradient was caused by abnormal inputs from the cochlea, we used diphtheria toxin receptor (DTR) mice in which hair cells can be selectively ablated (Tong et al., 2011; Golub et al., 2012). These mice show no cell size gradient after hair cells were ablated suggesting auditory activity is necessary to maintain the gradient. We also show the gradient can return after a period of auditory deprivation suggesting changes in cell size are plastic and reversible.

In addition to a cell size gradient, there are gradients of ion channels along the tonotopic axis in the MNTB (von Hehn et al., 2004; Leao et al,. 2006; Gazula et al, 2010). We used ICC to determine if PMCA2 is homogenously expressed throughout the MNTB. While total PMCA2 is greater in lateral cells than medial cells, this is due to the cell size gradient. The density of PMCA2 is homogenous along the tonotopic axis. Additionally, we show auditory activity does not affect the density of PMCA2 in the MNTB.

In summary, PMCA2 is highly expressed in the MNTB, there is a cell size gradient in the MNTB that requires auditory activity, and homogenous expression of PMCA2 in the MNTB is not affected by auditory inputs.

## Table of Contents

*Page*

## List of Figures

List of tables

## Abbreviations

| | |
|---|---|
| aCSF | artificial CSF |
| AMPA | α-amino-3-hydroxy-5-methyl-4-isoxazolepropionic acid |
| ATP | adenosine triphosphate |
| BL/6 | C57BL/6 mouse strain |
| $C_m$ | capacitance of the membrane |
| CN | cochlear nucleus |
| DT | diphtheria toxin |
| *dfw* | *deafwaddler* |
| DTR | diphtheria toxin receptor |
| EPSC | excitatory post synaptic current |
| g | grams |
| GBC | globular bushy cells |
| HCN4 | hyperpolarization-activated cyclic nucleotide-gated channel 4 |
| ΔI | current difference |
| ICC | immunocytochemsitry |
| IID | interaural intensity difference |
| ITD | interaural time difference |
| LSO | lateral superior olive |
| MAP2 | microtubule associated protein 2 |
| MΩ | mega-ohms |
| mV | millivolts |
| µm | micrometer |
| µM | micromolar |

| | |
|---|---|
| MNTB | medial nucleus of the trapezoid body |
| MSO | medial superior olive |
| NMDA | N-methyl-D-aspartate |
| PBS | phosphate buffered solution |
| PMCA2 | plasma membrane calcium ATPase 2 |
| $R_a$ | electrode resistance |
| $R_i$ | input resistance |
| $R_m$ | resistance of the membrane |
| ROI | region of interest |
| SBC | spherical bushy cells |
| SOC | superior olivary complex |
| $\tau$ | time constant |
| TTX | tetrodotoxin |
| $\Delta V$ | voltage of the command step |
| VGCC | voltage gated calcium channel |
| VGLUT1 | vesicular glutamate transporter 1 |

**Acknowledgements**

I would like to take this opportunity to thank Bruce Tempel for his support and guidance as my mentor. I would also like to thank my committee William Catterall, Sandra Bajjalieh, Sheri Mizumori, and Edwin Rubel for their input and guidance through my graduate career. I would like to give special thanks to Edwin Rubel for his guidance and support in designing the histology experiments and providing me with tissue for the gerbil experiments. I would like to acknowledge the Auditory Neuroscience Training Grant for three years of support. Thanks to Yuan Wang, Carol Robbins, and Glen McDonald for teaching me ICC, tissue collection, and imaging respectively. Thanks to Ling Tong for teaching me IM injections and providing me with DTR tissue for preliminary experiments. Thanks to Thomas Pasic for the use of the gerbil tissue used for all of the gerbil experiments. Thanks to Linda Robinson for her husbandry work and making sure I always had the mice I needed when I needed them. Thank you to Conny Kopp-Scheinpflug and Ian Forsythe for doing the capacitance experiments and their input in to the cell size gradient manuscript. Thanks to Valarie Street for her help with the cell size gradient manuscript. Thank you to Jenny Thornton for her help with the line scan data.

Thanks to everyone else in the Tempel lab. Jin Li, Claire Watson, Braulio Peguero, and Rebecca Minch for your input and encouragement throughout my graduate career.

Thanks to my mother, Glenda Hill, for always believing in me and supporting me even when I get in over my head. Thanks to my daughter Emma Weatherstone for giving me a reason to do what I do. And most importantly, thank you to my husband Ryan for being my biggest supporter over the last 6 years. I could not have done this without you.

## Dedication

To Emma Rose, my reason for being.

# Chapter 1

## Introduction

For organisms to survive, they must be able to interpret stimuli from their environment to find food, mate, and avoid prey. The visual system detects light waves, the olfactory and gustatory systems detect chemical signals, the somatosensory system detects temperature and touch, and the auditory system detects sound. All of these systems take stimuli from the environment and translate them into electrochemical signals that are processed in the brain in to what we perceive as the five senses. The mammalian auditory system is able to translate sound waves in to electrochemical signals that we perceive as sound. It is important that the auditory system not only detect that a sound is present, but also give the organism information about that sound. The wavelength of the sound perceived as pitch and the amplitude is perceived as intensity. In addition to giving information about the sound wave itself, it is important that the organization is able to perceive from where the sound originated. To fully understand how the brain is able to localize sound we must investigate how the brain functions from a systems level all the way down to the molecular level. At the molecular level, there are many important

proteins that are necessary for hearing and sound localization. One of the proteins that has been identified is the plasma membrane calcium ATPase 2 (PMCA2). PMCA2 pumps calcium from inside the cell to the extracellular space. PMCA2 is one mechanism of calcium clearance that allows the cell to regulate calcium concentrations. In this thesis we examine where PMCA2 is localized in neurons involved in sound localization and investigate how auditory activity affects PMCA2 expression in these neurons.

*1.1 Sound localization and the auditory brainstem*

The mammalian brain uses interaural time differences (ITD), interaural intensity differences (IID), and monaural spectral shape cues to localize sound. ITDs and IIDs are used to localize sound in azimuth while monaural spectral shape cues give information about sound localization in the vertical plane.

ITDs are defined as the difference in arrival time of the sound between the ears. If a sound originates from directly in front of the subject, the sound will arrive at both ears simultaneously and the ITD will be zero. Conversely, if the sound comes from directly to the right of the subject, the sound will reach the right ear before it reaches the left ear with the maximum ITD. IIDs are the difference in sound pressure level of the sound reaching the two ears. Because the head has a shadowing effect, the sound will be louder in the ear that is closer to the sound than in the ear that is farther from the sound.

Historically, it was thought that low frequency sounds were localized using ITDs while high frequency sounds were localized using IIDs (Rayleigh, 1907). These two binaural cues were also thought to be processed by two separate neural pathways in the superior olivary complex (SOC). The medial and lateral superior olives (MSO and LSO) were thought to process

ITDs and IIDs respectively. Recent data show that this dichotomy is not as strict as originally thought and that the LSO can respond to ITDs as well as IIDs (Tollin and Yin, 2005) although it is still considered to be the initial site of IID processing.

For the LSO to process IIDs it must receive binaural inputs. Sound transduction begins in the periphery where hair-cells transform sound from a mechanical signal to an electrochemical signal. This electrochemical signal is sent as an action potential from spiral ganglion cells to the cochlear nucleus (CN). Spherical bushy cells (SBC) in the CN send excitatory signals to the ipsilateral LSO, while globular bushy cells (GBC) in the CN send excitatory signals to the contralateral medial nucleus of the trapezoid body (MNTB). The MNTB inverts this signal from excitatory (glutamatergic) to inhibitory (glycinergic). This inhibitory signal is sent from the MNTB to the LSO that is contralateral to the origin of the stimuli. The LSO compares excitatory signals originating in the ipsilateral cochlea with inhibitory signals originating in the contralateral cochlea (von Gersdorff and Borst, 2002)(Figure 1.1).

Although temporally precise inputs are not required for IID sensitivity during a sustained response, timing is important for IID sensitivity at stimulus onset (Grothe and Park 1995; Irvine et al, 2001). At the LSO, inhibitory inputs coming from the MNTB are subtracted from the excitatory inputs coming from the CN (Moore and Caspary, 1983). The inhibitory inputs have to travel further and have an additional synaptic stage at the MNTB so one might expect this signal to arrive later than the signal coming from the ipsilateral CN. However, the inhibitory pathway is able to compensate for this delay because the axon diameter of GBCs is larger than in SBCs (Schwartz, 1992) and there is minimized synaptic delay at the MNTB synapse (von Gersdorff and Borst, 2002). In addition to minimizing synaptic delay, MNTB neurons must fire precisely such that the temporal information is conserved throughout the circuit (Grothe and Park 1995;

Wang et al., 1998; Taschenberger and von Gersdorff, 2000). MNTB neurons must also be able to fire quickly. These neurons have firing rates of more than 300 spikes per second *in vivo* (Kopp-Scheinpflug et al., 2008). It is clear that MNTB neurons have a very specialized task and must have special properties to be able to minimize synaptic delay and maximize precision while maintain fast firing rates. To maintain precision and speed, one would expect that residual calcium must be cleared to avoid either synaptic facilitation or depression, therefore MNTB neurons must possess an efficient calcium clearance mechanism. We hypothesize that plasma membrane calcium ATPase 2 (PMCA2), the most efficient of the plasma calcium ATPases, plays an important role in this calcium clearance.

*1.2 A model for synaptic transduction in the MNTB*

MNTB neurons have unique characteristics that scientists have taken advantage of when studying synaptic function. Morphologically these neurons consist of a large principal cell with synaptic fingers surrounding the cell forming around 600 synaptic sites (Forsythe, 1994). These finger like projections are called the calyx of Held. Because there are so many synaptic sites on each neuron, it is possible to record the pre-potential as well as the post-synaptic potential using an extracellular recording electrode. This unique property has led scientists to use MNTB neurons to study synaptic function and in return much is known about MNTB neuron physiology.

Our current understanding of how the MNTB synapse works is that as action potentials are sent from the CN and reach the synapse at the MNTB, this change in voltage opens voltage gated calcium channels (VGCC) at the active sites in the calyx of Held. Calcium rushes in to the cell and stimulates exocytosis of vesicles containing glutamate. Glutamate enters the synaptic cleft

and binds to α-amino-3-hydroxy-5-methyl-4-isoxazolepropionic acid (AMPA) receptors on the post-synaptic membrane of the principal cell. AMPA receptors are ionotropic receptors permeable to calcium and sodium. Glutamate is also the neurotransmitter that binds to N-methyl-D-aspartate (NMDA) receptors. Although there are NMDA receptors in the MNTB of during development, by adulthood (4wks) there are very few if any NMDA receptors in the MNTB and the contribution of NMDA receptors to the excitatory post synaptic current (EPSCs) is negligible (Futai et al, 2001). For the purpose of this thesis we will focus on glutamate binding exclusively to AMPA receptors.

When glutamate binds these AMPA receptors they open and allow calcium and sodium to rush in to the principal neuron. This triggers an action potential in the principal cell that is sent down the axon to the LSO. Calcium in the calyx of Held inactivates VGCC stopping calcium from entering the calyx of Held preventing more glutamate from being released (Figure 1.2). Because calcium is responsible for triggering exocytosis , partially carrying the charge of the post-synaptic action potential, and inactivating VGCC, it's presence must be tightly regulated in order for synaptic transduction to function properly.

*1.3 Calcium Clearance Mechanisms in the MNTB*

It is estimated that in a typical neuron, the intracellular calcium concentration is 0.0001μM as compared to the extracellular calcium concentration of 2μM. It is crucial that neurons maintain this concentration gradient so that calcium is able to flow unfacilitated through calcium channels when they open. Maintaining a low level of cytoplasmic calcium also allows the cell to be sensitive to calcium serving as a second messenger. To keep intracellular calcium concentrations low, cells have developed multiple calcium clearance mechanisms. These calcium clearance

mechanisms include endogenous calcium buffers, pumping calcium in to intracellular stores, and clearing calcium in to the extracellular space. The plasma membrane calcium ATPases (PMCAs) are one way cells are able to clear calcium from the cytoplasm in to the extracellular space. PMCAs use adenosine triphosphate (ATP) to pump calcium from the intracellular space to the extracellular space therefore keeping intracellular calcium concentrations relatively low compared to the extracellular calcium concentrations.

### *1.4 PMCA2 localization*

There are four types of PMCAs, PMCA1-4. PMCA1 and PMCA4 are ubiquitously expressed while PMCA2 and PMCA3 are the main PMCAs expressed in the central nervous system (Carafoli and Stauffer, 1994). Each PMCA can be alternatively spliced at two sites A and C (Strehler et al, 1989; Heim et al, 1992; Keeton et al, 1993). Site A is thought to control if PMCA is localized to the apical or basolateral membrane in polarized cells (Hill et al., 2006; Antalffy et al., 2012). Site C affects PMCAs ability to interact with calmodulin which alters the kinetics of the pump when bound (Keeton et al., 1993; Hilfiker et al., 1994; Caride et al., 2007). PCMA2 is the most efficient of the PCMAs (Brini et al., 2003) and is the focus of this thesis.

PMCA2 mRNA is found in the heart, liver, kidney, spleen, mammary gland, retina, and inner ear (Keeton et al., 1993; Silverstein and Tempel, 2006). Although PMCA2 is ubiquitously expressed, it is highly expressed in retina (Krizaj et al., 2002; Renteria et al, 2005) and Purkinje neurons (Stahl et al., 1992) as well as auditory and vestibular hair cells.

Mice and humans with mutations in the gene for PMCA2 have hearing and vestibular phenotypes highlighting PMCA2's critical role in the auditory and vestibular systems (Street et

al., 1994; Kozel et al., 1998; Takahashi and Kitamura, 1999; McCullough and Tempel, 2004; Schultz et al., 2005; Spiden et al., 2008; Bortolozzi et al., 2010; Watson and Tempel, 2013)

PMCA2 has largely been studied in the mammalian auditory system although most research has focused on PMCA2 in hair cells. PMCA2 is highly expressed in hair cells and is localized to the stereocillia (Dumont et al., 2001; Furuta et al., 1998; Wood et al., 2004). PMCA2 is also expressed in the spiral ganglion neurons that innervate these hair cells (Kozel et al, 1998; Yamoah et al, 1998).

*1.5 PMCA2 mutants as a tool for studying PMCA2 in the auditory brainstem*

PMCA2 is encoded by the *Atp2b2* gene in mice. Spontaneous mutations have occurred in *Atp2b2* that allow us to study PMCA2 function. The first PMCA2 mutant that was discovered was the *deafwaddler* (*dfw*) mutant (Street et al., 1998). This mutant gets its name because the mutation causes hearing and vestibular problems resulting in a homozygous mutant that is deaf and has a wobbly gait. The *dfw* mutation is a point mutation that renders the PMCA2 pump less efficient that wildtype. Biochemical assays suggests that PMCA2 protein resulting from this mutation pump at about 30% efficiency compared to wildtype (Penheiter et al., 2001) (Table 1). Another mutation that has occurred in mice is the $dfw^{2J}$ mutation. This mutation is a two nucleotide deletion that results in a premature stop codon (Street et al., 1998). This is a null mutation and homozygous mutants produce no PMCA2 protein (McCullough and Tempel, 2004). $dfw^{2J}$ heterozygotes (+/$dfw^{2J}$) show some up regulation of PMCA2 and produce about 60% PMCA2 protein compared to wildtype (Watson et al., 2013). +/$dfw^{2J}$ have high frequency hearing loss while homozygotes ($dfw^{2J}$/ $dfw^{2J}$) are completely deaf and ataxic (McCullough and

Tempel, 2004). These mutants allow us to study the range of PMCA2 function ranging from 0% to 100% (Table 1).

*1.6 Ion channel gradients in the MNTB*

Like many auditory nuclei, the MNTB is arranged tonotopically with medial cells responding best to high frequency sounds and lateral cells responding best to high frequency sounds (Sonntag et al., 2009). Ion channel gradients have been discovered in the MNTB. Kv3.1 is a voltage-sensitive potassium channel. In 2001 Li et al. used immunolabeling to show that Kv3.1 labeling varied across the tonotopic axis of the MNTB of rat with medial neurons showing more intense labeling that lateral neurons (Figure 1.3A). von Hehn et al. followed up this study by showing this gradient also existed in normal hearing CBA/J mice. To study how auditory activity affected Kv3.1 expression they used C57BL/6 (BL/6) mice which show age related hearing loss. In young BL/6 mice with normal hearing, there was a gradient of Kv3.1. By 8 months old, the BL/6 mice showed significant hearing loss and the gradient of Kv3.1 was abolished. In 8mo old, normal hearing CBA mice, the gradient remained. These data suggested that auditory activity was required to maintain the Kv3.1 gradient (Figure 1.3B).

In 2006, Leao et al., used both immunohistochemical labeling and patch-clamp recordings to show a medial to lateral gradient of Kv1.1, a low threshold voltage-sensitive potassium channel, and a lateral to medial gradient of hyperpolarization-activated cyclic nucleotide-gated channel 4 (HCN4) (Figure 1.3A). They also used the *dn/dn* mouse, a congenitally deaf mouse, as a deaf mouse model showing auditory activity was required to maintain the gradients of these channels in the MNTB (Figure 1.3B). Interestingly, they note that in their deaf mouse model, the ion channel concentrations revert to the level seen in medial cells of hearing mice.

In 2010 Gazula et al. examined expression of Kv1.3, another voltage-dependent potassium channel, in the MNTB. Using immunocytochemistry they found that Kv1.3 was more highly expressed in lateral cells than medial cells (Figure 1.3A). To date there are no data determining if Kv1.3 expression is affected by auditory activity (Figure 1.3B).

The membrane composition of MNTB neurons is complex and hard to study in part because composition changes along the tonotopic axis. Adding to the complexity, MNTB neurons change the composition ion channels as they mature. Compiling the data from different groups using different methods makes it difficult to draw true conclusions about the role of these ion channel gradients, but the data show there are multiple ion channels that are differentially expressed along the tonotopic axis. Many of these gradients also require auditory activity (Figure 1.3). These findings suggest MNTB neurons may be able to subtly change their firing properties based on stimulation. In this thesis we will examine patterns of PMCA2 expression in the MNTB and determine if auditory activity affects their expression.

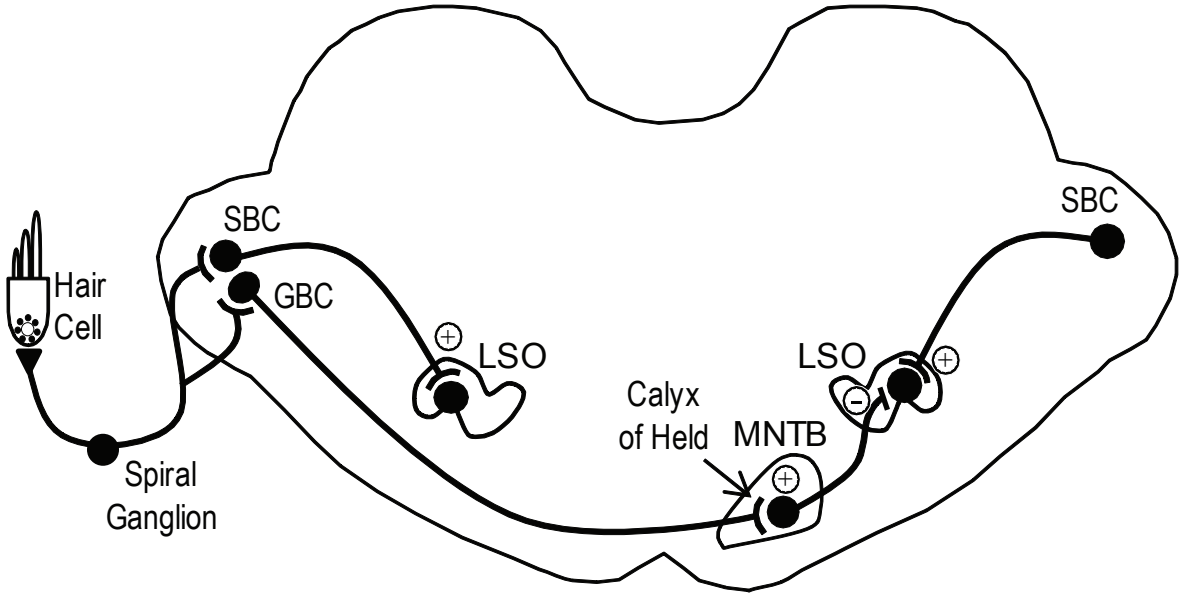


**Figure 1.1. Superior olivary complex circuitry.** Sound transduction begins in the hair-cell stereocilia, which transform sound from a mechanical signal to an electrochemical signal. This electrochemical signal is sent as an action potentials from spiral ganglion cells to the cochlear nucleus (CN). Spherical bushy cells (SBC) in the CN send excitatory signals to the ipsilateral lateral superior olive (LSO), while globular bushy cells (GBC) in the CN send excitatory signals to the contralateral medial nucleus of the trapezoid body (MNTB). The MNTB inverts this signal from excitatory (glutamatergic) to inhibitory (glycinergic). This inhibitory signal is sent from the MNTB to the LSO that is contralateral to the origin of the stimuli. The LSO compares excitatory signals originating in the ipsilateral cochlea with inhibitory signals originating in the contralateral cochlea. (Figure adapted from von Gersdorff and Borst, 2002.)

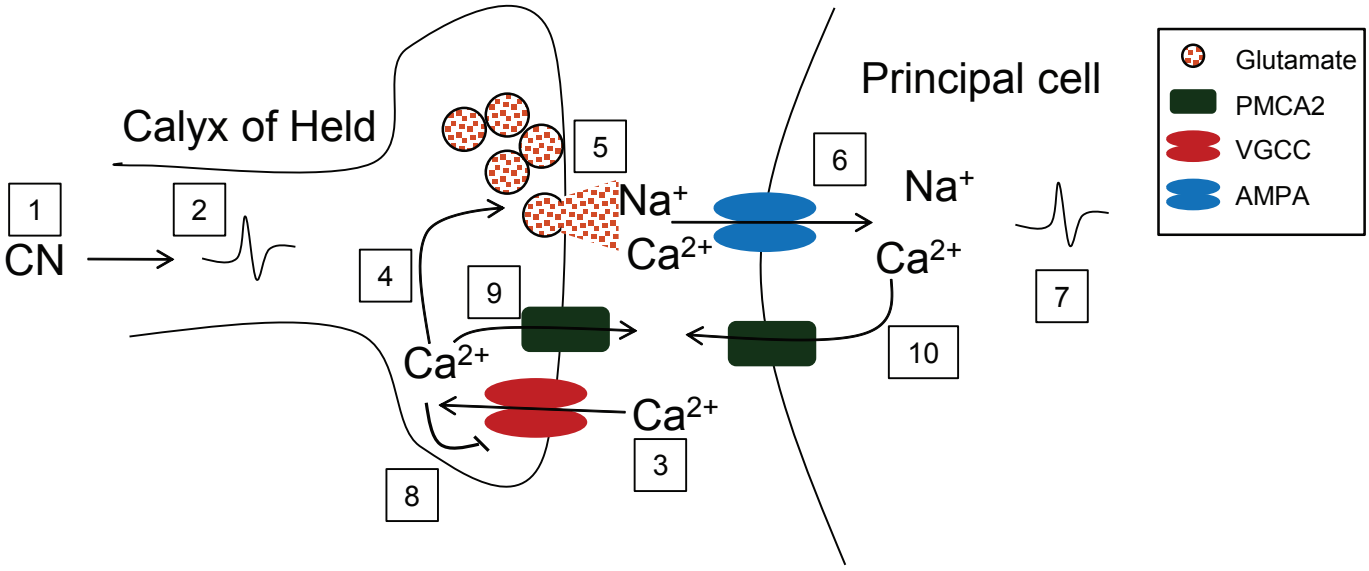


**Figure 1.2 Model of calcium flow in an MNTB neuron.** (1) Action potentials are generated in the cochlear nucleus (CN) and (2) reach the synapse at the medial nucleus of the trapezoid body (MNTB). (3) This change in voltage opens voltage gated calcium channels (VGCC) at the active sites in the calyx of Held. (4) Calcium ($Ca^{2+}$) rushes in to the cell and stimulates exocytosis of vesicles containing glutamate. (5) Glutamate enters the synaptic cleft and binds to α-amino-3-hydroxy-5-methyl-4-isoxazolepropionic acid (AMPA) receptors on the post-synaptic membrane of the principal cell. (6) AMPA receptors they open and allow $Ca^{2+}$ and sodium ($Na^{+}$) to rush in to the principal neuron. (7) This triggers an action potential in the principal cell. (8) $Ca^{2+}$ in the calyx of Held inactivates VGCC stopping $Ca^{2+}$ from entering the calyx of Held preventing more glutamate from being released. We propose that if plasma calcium ATPase 2 (PMCA2) is present in these neurons it could clear calcium from (9) the calyx of Held, (10) the principal cell, or both.

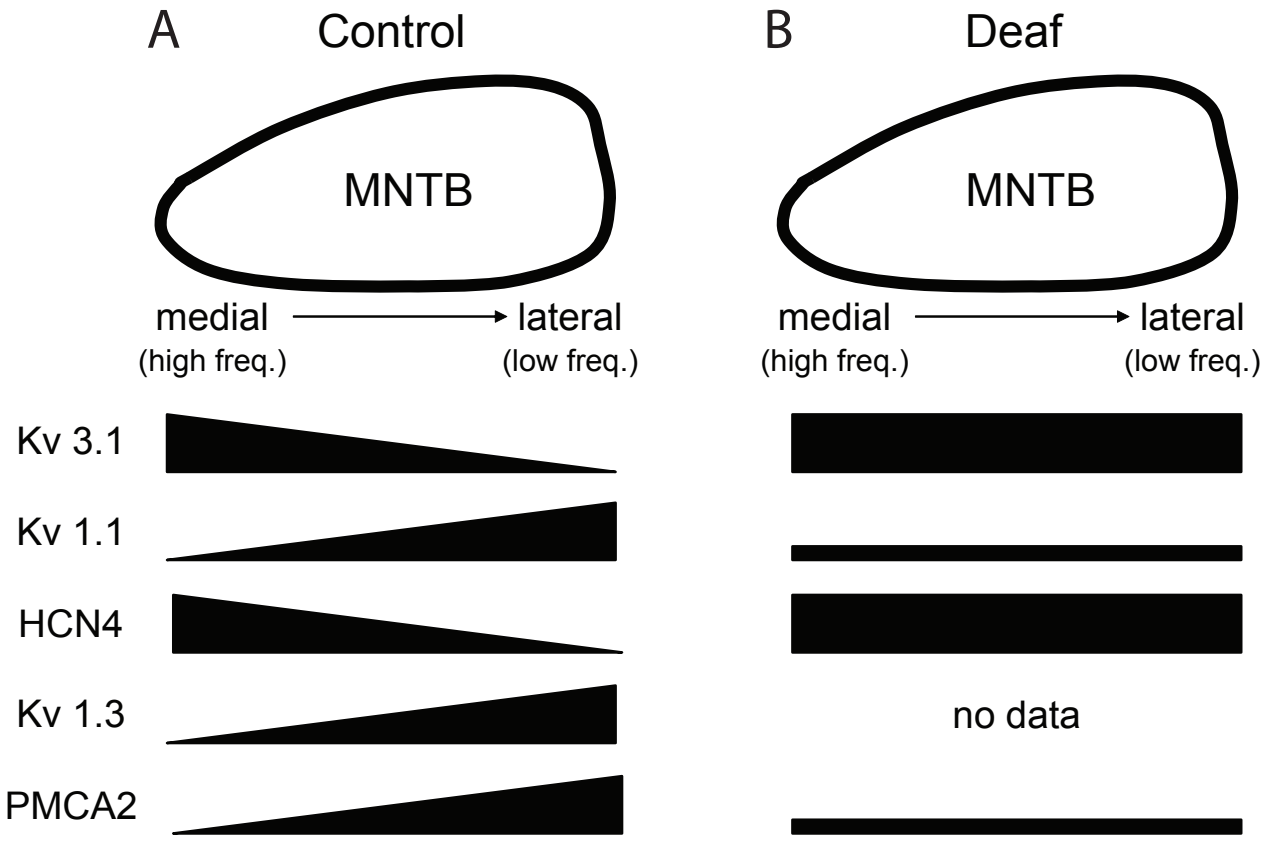


**Figure 1.3 Summary of gradients of ion channels in the MNTB**
A) In normal mice, Kv3.1 (Li et al., 2001 (rat); von Hehn et al., 2004 (mouse)) and HCN2 (Leao et al., 2006) channels show a medial to lateral concentration gradient while Kv1.1 (Leao et al., 2006) and Kv1.3 (Gazula et al., 2010) channels are more highly expressed in lateral cells than medial cells. This thesis will examine PMCA2 expression along the tonotopic axis in the MNTB. We show that total PMCA2 is expressed more highly in lateral cells compared to medial cells. B) In deaf mice, all of these gradients are abolished and expression levels change to match the level of expression in medial cells. (Li et al., 2001; von Hehn et al., 2004; Leao et al., 2006; Strumbos et al., 2010) Figure adapted from Leao et al., 2006.

**Table 1. PMCA2 function in *deafwaddler* mutants and DTR mice**

| Genotype | Hearing Phenotype | PMCA2 Protein | PMCA2 Efficiency | Total PMCA2 function |
|---|---|---|---|---|
| Wild type | normal | 100% | 100% | 100% |
| *dfw*$^{2J}$ +/- | High frequency loss | ~60% | 100% | ~60% |
| *dfw* -/- | deaf | 100% | ~30% | ~30% |
| *dfw*$^{2J}$ -/- | deaf | 0% | 0% | 0% |
| DTR | deaf | 100% | 100% | 100% |

# Chapter 2

## PMCA2 localization in the Auditory Brainstem


### Summary

The plasma membrane calcium ATPase 2 (PMCA2) pumps calcium from inside the cell to the extracellular space. It is known that PMCA2 is present in neurons involved in sound localization of the chick auditory brainstem (Wang et al., 2009), but PMCA2 has not been well characterized in the mammalian auditory brainstem. We show that PMCA2 is present in the medial nucleus of the trapezoid body (MNTB), cochlear nucleus (CN), and lateral superior olive (LSO). Morphologically, MNTB neurons consist of the calyx of Held which wraps around MNTB principal cells forming approximately 600 active sites in the post-synaptic cell body. Understanding if PMCA2 is expressed in calyx, principal cell, or in both is essential to understanding PMCA2's role in the MNTB. Using immunocytochemistry (ICC) we characterize the pre- and post-synaptic expression of PMCA2 in these neurons.

## 2.1 Introduction

One way the mouse localizes sound is by calculating interaural intensity differences (IID). Sound transduction begins in the hair-cell stereocilia, which transform sound from a mechanical signal to an electrochemical signal. This electrochemical signal is sent as an action potential from spiral ganglion cells to the CN. Spherical bushy cells (SBC) in the CN send excitatory signals to the ipsilateral LSO, while globular bushy cells (GBC) in the CN send excitatory signals to the contralateral MNTB (Figure 1.1). The MNTB inverts this signal from excitatory (glutamatergic) to inhibitory (glycinergic). This inhibitory signal is sent from the MNTB to the LSO that is contralateral to the origin of the stimuli. The LSO compares excitatory signals originating in the ipsilateral cochlea with inhibitory signals originating in the contralateral cochlea.

Because neurons in the MNTB have a very specialized task, they have a unique morphology and electrophysiological properties. Morphologically, each MNTB principal neuron is innervated by a single CN bushy cell axon with fingerlike projections that wrap around a the cell body forming ~600 synaptic release sites on the post-synaptic MNTB neuron (Forsythe 1994). Neurons in the MNTB fire with great speed and precision (Wang et al., 1998; Taschenberger and von Gersdorff, 2000), characteristics for which rapid calcium clearance is essential. MNTB neurons have firing rates of more than 300 spikes per second (Kopp-Scheinpflug et al., 2008), and the calcium that enters during each action potential must be quickly removed to enable the next action potential. Because the LSO compares arrival times of action potentials sent from the MNTB to arrival times of action potentials sent from the CN, MNTB neurons must fire precisely such that the temporal information is conserved throughout the circuit. To maintain precision, residual calcium must be cleared to avoid either synaptic

facilitation or depression. It is clear that the specialized function of the MNTB requiring rapid yet precise action potentials must be accompanied by an efficient calcium clearance mechanism. We show that PMCA2 is present in the MNTB and adjacent nuclei suggesting it plays a role in calcium clearance in MNTB neurons.

**2.2 Methods**

*Animals.* Adult (5-7 week old) CBA or CBA/CaJ deafwaddler (*dfw*$^{2J}$) mice of either sex were obtained from the University of Washington Tempel Lab breeding colony. All manipulations were carried out in accordance with protocols approved by the University of Washington Animal Care Committee.

*Histology.* The animals were anesthetized with Nembutal and perfused with a saline-heparin solution followed by 4% paraformaldahyde. The brains were exposed in the skull and stored in 4% paraformaldahyde overnight. The brains were then dissected from the skull and post-fixed for an additional hour. The tissue was transferred to 10% sucrose in 0.1M phosphate buffer until sinking which took approximately 3 hours. The tissue was transferred again to 30% sucrose in 0.1M phosphate buffer where they remained until sinking, which took approximately 24 hours. Coronal sections 10 or 40 μm thick were cut through the brain stem using a freezing microtome. The free floating sections were stored in phosphate-buffered saline (PBS; pH 7.4).

*Immunocytochemistry.* The fixed floating sections were treated with primary antibody for PMCA2 at a dilution of 1:250 in PBS with 0.3% Triton X-100 for 2 hours at room temperature. The sections were washed in PBS overnight at 4°C. The sections were then incubated with microtubule associated protein 2 (MAP2) primary antibody and/or vesicular glutamate transporter 1 (VGLUT1) primary antibody for 1.5 hours at room temperature. MAP2 was diluted

at 1:1000 in PBS with 0.3% Triton X-100. VGLUT1 was diluted at 1:500 in PBS with 0.3% Triton X-100. The sections were washed in PBS before incubating in AlexaFlour secondary antibodies (1:200; Molecular Probes, Eugene, OR) for 2 hours at room temperature. Some sections were treated with DAPI before the coverslip was applied.

*Primary Antibodies.* Polyclonal anti-PMCA2 (catalog No. PA1-915) made in rabbit was purchased from Affinity Bioreagents (Golden, CO). The immunogen is a synthetic peptide corresponding to amino acid residues 5-19 of human PMCA2 protein. The sequence of the immunogen is TNSDFYSKNQRNESS. This sequence is completely conserved between human and mouse PMCA2. Monoclonal anti-MAP2 (catalog No. MAB3418) made in mouse was purchased from Chemicon International. The immunogen is bovine brain microtubule protein. The antibody binds specifically to MAP2a and MAP2b. Guinea pig polyclonal antiserum anti-VGLUT1 ( catalog No. 135 304) was purchased from Synaptic Systems (Gottingen, Germany).

*Confocal Microscopy.* Images were taken with an Olympus FV-1000 Confocal microscope. The MNTB was identified by its characteristic location and shape. MNTB neurons were identified by their characteristic morphology. For all images a z-stack was taken and deconvolved using the Huygens deconvolution system. The image was cropped, brightness and contrast were adjusted to maximize visualization.

*Line Scans*. Line scans were performed in which the average fluorescence was calculated along a line that spanned the intracellular space of the principal cell and across the calyx of Held. A total of four cells and 12 line scans were analyzed. Peaks for each channel were defined as maximum intensity where intensity never increased again for that channel moving in the direction of the intersection (L→R and R→L for MAP2 and VGLUT1 respectively in figure 2.4B). To determine if PMCA2 was closer to the pre– or post-synaptic marker we used two

different measurements to estimate the center of the synaptic cleft. The location where MAP2 and VGLUT1 intersected (intersection) and the median of the distance between peaks for MAP2 and VGLUT1 (median). The distance from PMCA2 to the intersection and median was calculated for all line scans.

## 2.3 Results

### *2.3.1 PMCA2 is present in the MNTB*

ICC experiments demonstrated that PMCA2 is expressed throughout the MNTB. Wildtype MNTB show labeling for PMCA2 throughout the MNTB (Figure 2.1A-C) while $dfw^{2J}/dfw^{2J}$ MNTB, which lack PMCA2, show only background staining (Figure 2.2D-F) indicating that our antibody correctly binds to PMCA2 protein.

### *2.3.2 PMCA2 is present in the CN and LSO*

The major nuclei that connect to the MNTB in the auditory brainstem circuit are the CN and LSO. ICC experiments demonstrated that PMCA2 is also expressed in these nuclei (Figure 2.2).

### *2.3.3 ICC suggests PMCA2 is localized both pre- and post-synaptically*

High resolution images showing PMCA2 with a pre-synaptic (Figure 2.3A-C) or post-synaptic (Figure 2.3D-F) marker. These images show what appear to be a cross sections through the calyx of held. Figure 2.3A shows labeling for VGLUT1, a pre-synaptic marker that fills the calyx of Held. PMCA2 labeling (Figure 2.3B) appears to be on both the inner and outer membrane of cross sections through calyx fingers suggesting PMCA2 is localized pre-synaptically. In areas where there is no VGLUT1 labeling, there still appears to be PMCA2

labeling suggesting that PMCA2 is also localized post-synaptically. Figure 2.3D shows labeling for MAP2, a somatodendritic marker that fills the post-synaptic cell and PMCA2 (Figure 2.3E). Figure 2.3F is a composite of MAP2 (green), PMCA2 (red), and DAPI (blue). The cross section through the calyx shows the inner and outer (arrows) membrane of the calyx. PMCA2 is clearly present in the outer membrane of the calyx indicating it is involved in pre-synaptic calcium clearance. PMCA2 is also present in the area where the inner calyx membrane and the post-synaptic membrane are located, but the resolution is not good enough to differentiate between the inner membrane of the calyx and post-synaptic membrane of the principal cell. It appears there is PMCA2 in the cytoplasm of the post-synaptic cell but it is not clear if this PMCA2 is transported to the post-synaptic membrane of the principal cell or is shipped down the axon to the pre-synaptic membrane of the synapse in the LSO (Figure 1.1), or both.

Although we see PMCA2 expression on the inner membrane of the calyx of Held, the resolution is not good enough to determine if this PMCA2 is on the pre- or post-synaptic size. To resolve this, we performed consecutive line scans of MNTB neurons labeled with VGLUT, PMCA2, and MAP2 (Figure 2.4A). We defined the midline either by the median of peak-to-peak distance or as where VGLUT1 and MAP2 intersected (Figure 2.4B). To determine if we could resolve the span of the synapse we calculated peak-to-peak distance (Figure 2.4C). The average of peak-to-peak distance was 666nm (SEM=72nm). This distance is substantially larger than we would expect the synaptic cleft to be indicating that while this measurement can be used to determine a midline, it is not representative of spanning only the synaptic cleft. The average distance of the PMCA2 peak from the intersection was 43nm (SEM=24nm). The average distance of the PMCA2 peak from the median was 59nm (SEM=39nm). Both of these measurements are closer to the VGLUT1 (pre-synaptic) peak than the MAP2 (post-synaptic)

peak but were not more than one standard deviation away from zero which was our criteria for concluding PMCA2 was more highly expressed on one membrane rather than the other.

### 3.4 Discussion

PMCA2 is an important regulator of calcium. Since calcium is extremely important in neurotransmission, it is important that we understand where PMCA2 is expressed to fully understand how neurons function. It has been demonstrated that PMCA2 is present in auditory nuclei of the chick (Wang et al., 2009) but PMCA2 expression has not been investigated in the mammalian auditory brainstem nuclei. Neurons in the auditory brainstem circuit must be able to fire very rapidly while maintain precision. MNTB neurons fire up to 300sps in vivo (Kopp-Scheinpflug et al., 2008). In order for IIDs to be calculated in the LSO, MNTB neurons must fire precisely so that arrival time accurately represent arrival times of action potentials in the MNTB. If calcium concentrations are not tightly regulated, facilitation and depression could disrupt this delicate balance. An efficient calcium clearance mechanism must be present in these neurons in order to prevent unregulated facilitation or depression. Since PMCA2 is the most efficient of the calcium ATPases (Brini et al, 2003), we hypothesized that it may play a role in this calcium clearance. Here we show that PMCA2 is highly expressed in the MNTB as well as the nuclei on either side of the MNTB in the auditory brainstem circuit. PMCA2 expression in these nuclei indicates that PMCA2 probably plays a major role in calcium clearance in these neurons.

To understand how PMCA2 may affect the electophysiolgical behavior of these neurons, we must determine if PMCA2 is expressed pre-synaptically in the calyx of Held, post-

synaptically in the principal cell, or both. Using ICC we show that PMCA2 lines both the outer and inner membrane of the calyx of Held (Figure 2.3). This suggests that PMCA2 is expressed pre-synaptically although at this resolution it is difficult to determine if the PMCA2 in the inner membrane of the calyx is only on the pre-synaptic calyx or if it is also on the post-synaptic membrane of the principal cell. Evidence that PMCA2 is localized post-synaptically is provided in Figure 2.3A-C where PMCA2 is present even when VGLUT1, a pre-synaptic marker that fills the calyx, is not present. This is our best evidence that PMCA2 is localized on the membrane of the principal cell. We do see PMCA2 labeling inside the principal cell which indicates that PMCA2 protein is made in the principal cell, but if this protein is shipped to the post-synaptic sites opposite the calyx of held is yet to be determined. Because we see PMCA2 expression in the LSO, it is possible that all of this PMCA2 is shipped down the axon to where the MNTB neurons synapse with LSO neurons. Additional evidence supporting post-synaptic expression of PMCA2 is found in Figure 2.4. Consecutive line scans of ICC with labeling for MAP2, PMCA2, and VGLUT1 show that the peak for PMCA2 is intermediate between the peak for MAP2 and VGLUT1. We would expect the peak for PMCA2 to be shifted towards VGLUT1 if PMCA2 was only expressed pre-synaptically. While the average of the line scans are slightly shifted towards VGLUT1, this shift does not exceed one standard deviation. We would also expect a slight shift in this direction since VGLUT1 is expressed on the pre-synaptic membrane and MAP2 is expressed inside the cell body. These line scans do not have the resolution to definitively tell us if PMCA2 is expressed on the post-synaptic membrane, but they do not give us any reason to believe that PMCA2 is not expressed on the post-synaptic membrane. Images using electron microscopy are needed to definitively determine where PMCA2 is localized.

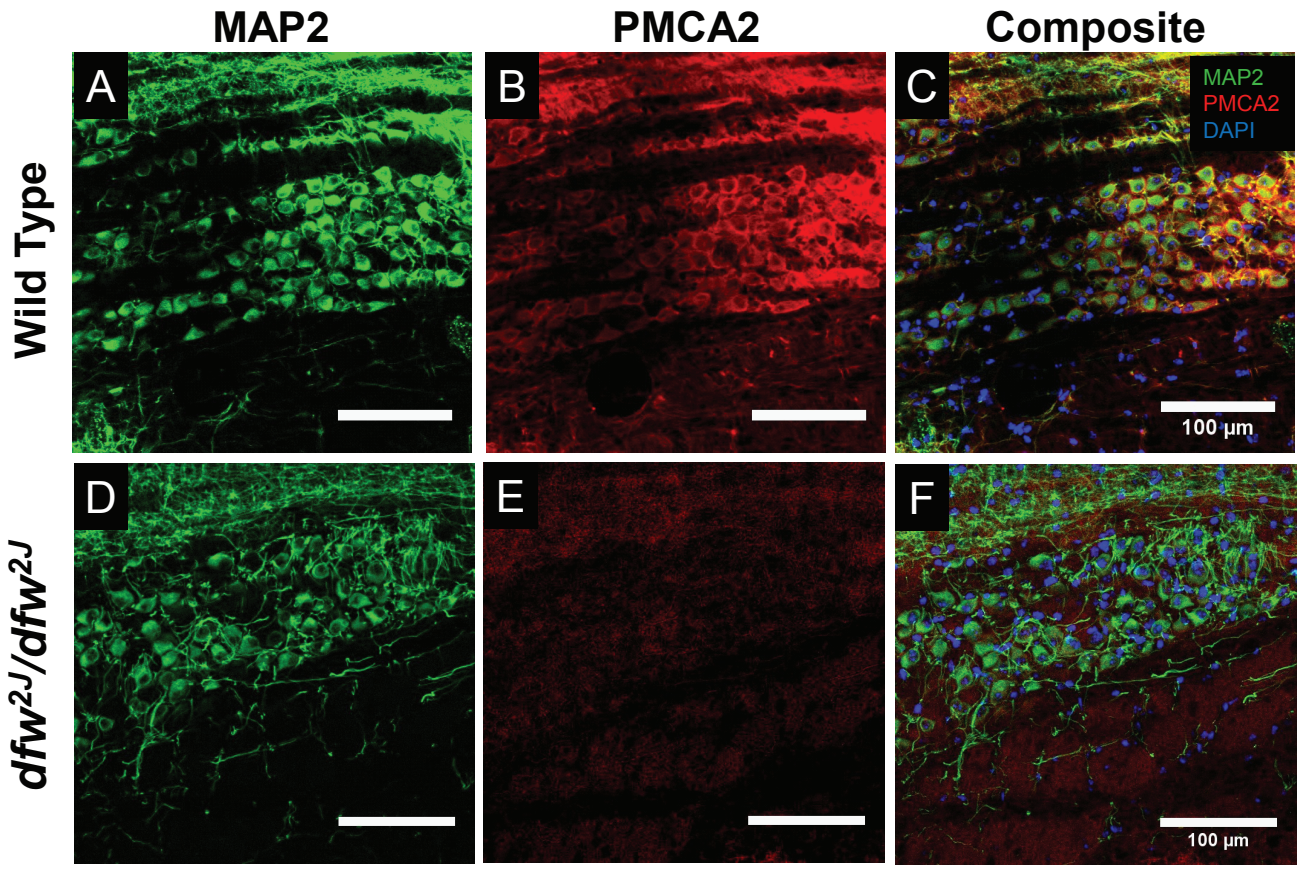


**Figure 2.1. PMCA2 in the MNTB.** ICC for A,D) MAP2 and B,E) PMCA2 in the MNTB of a wild type (A-C) or *dfw*$^{2J}$/ *dfw*$^{2J}$ (D-E) mouse. (Red=PMCA2, Green=MAP2, Blue=DAPI).

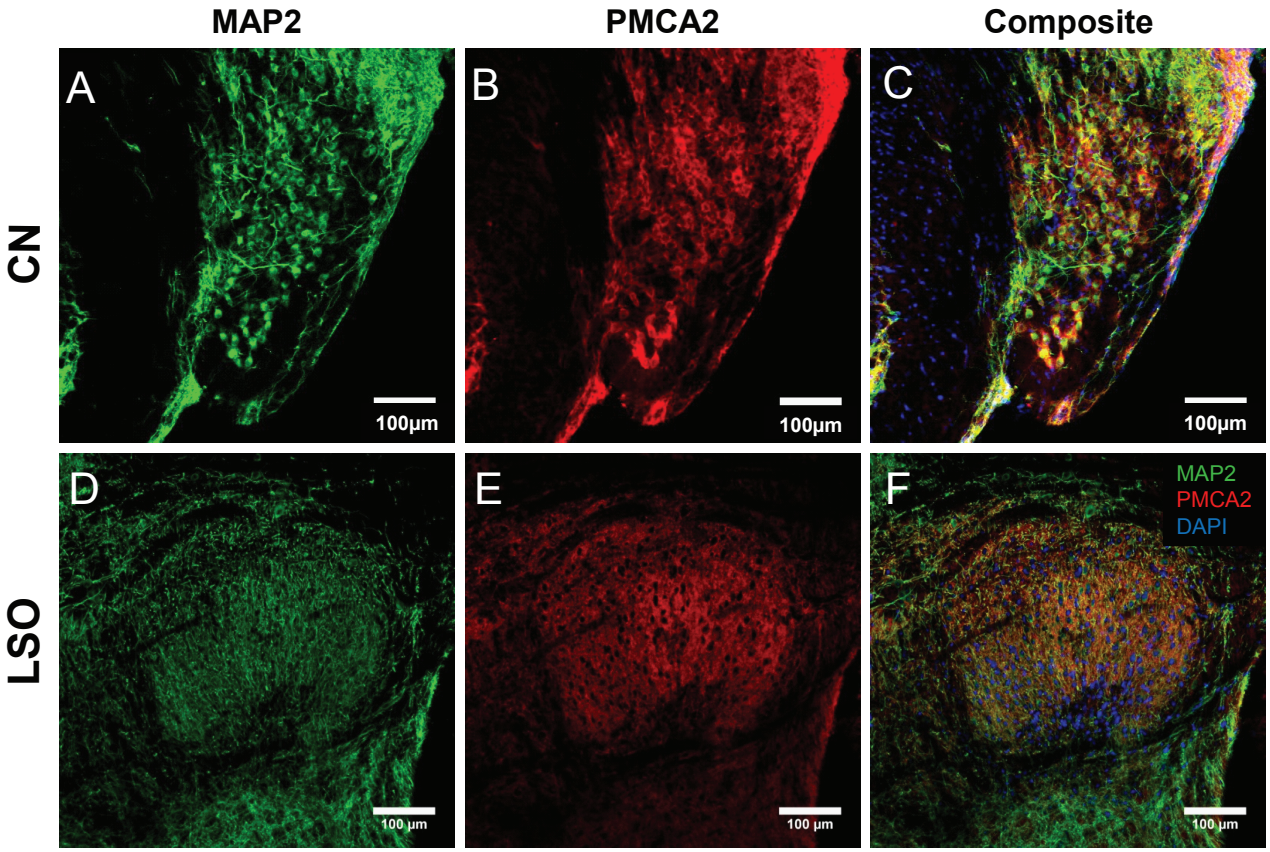


**Figure 2.2 PMCA2 in the CN and LSO**
ICC for A,D) MAP2 and B,E) PMCA2 in the CN (A-C) or LSO (D-E). (Red=PMCA2 Green=MAP2, Blue=DAPI).

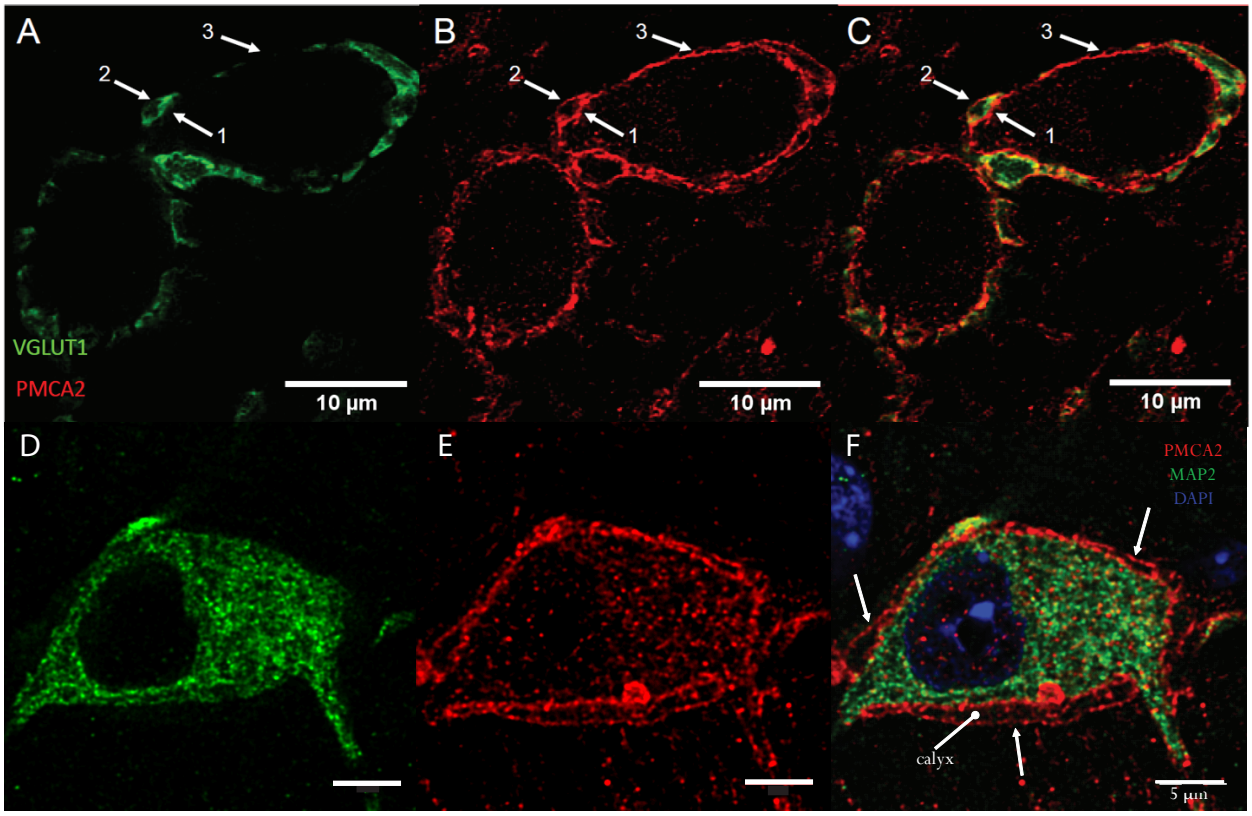


**Figure 2.3. ICC suggests PMCA2 is present on the pre– and post-synaptic membranes.** A) VGLUT1 (green) was used as a pre-synaptic marker to label the Calyx of Held along with B) PMCA2 (red). C) PMCA2 clearly surrounds the cross sections through the Calyx appearing to be present both on the pre-synaptic membrane (1) as well as the opposing membrane of the calyx finger (2). PMCA2 is also present in the absence of VGLUT1 suggesting PMCA2 may also be present on the membrane of the principal cell (3). D) MAP2 (green) a post synaptic marker and E) PMCA2 (red) in an MNTB neuron. F) A cross section through the calyx is marked 'calyx'. Arrows show where PMCA2 appears to be localized pre-synaptically in the outer membrane of the calyx. The nucleus is stained with DAPI (blue).

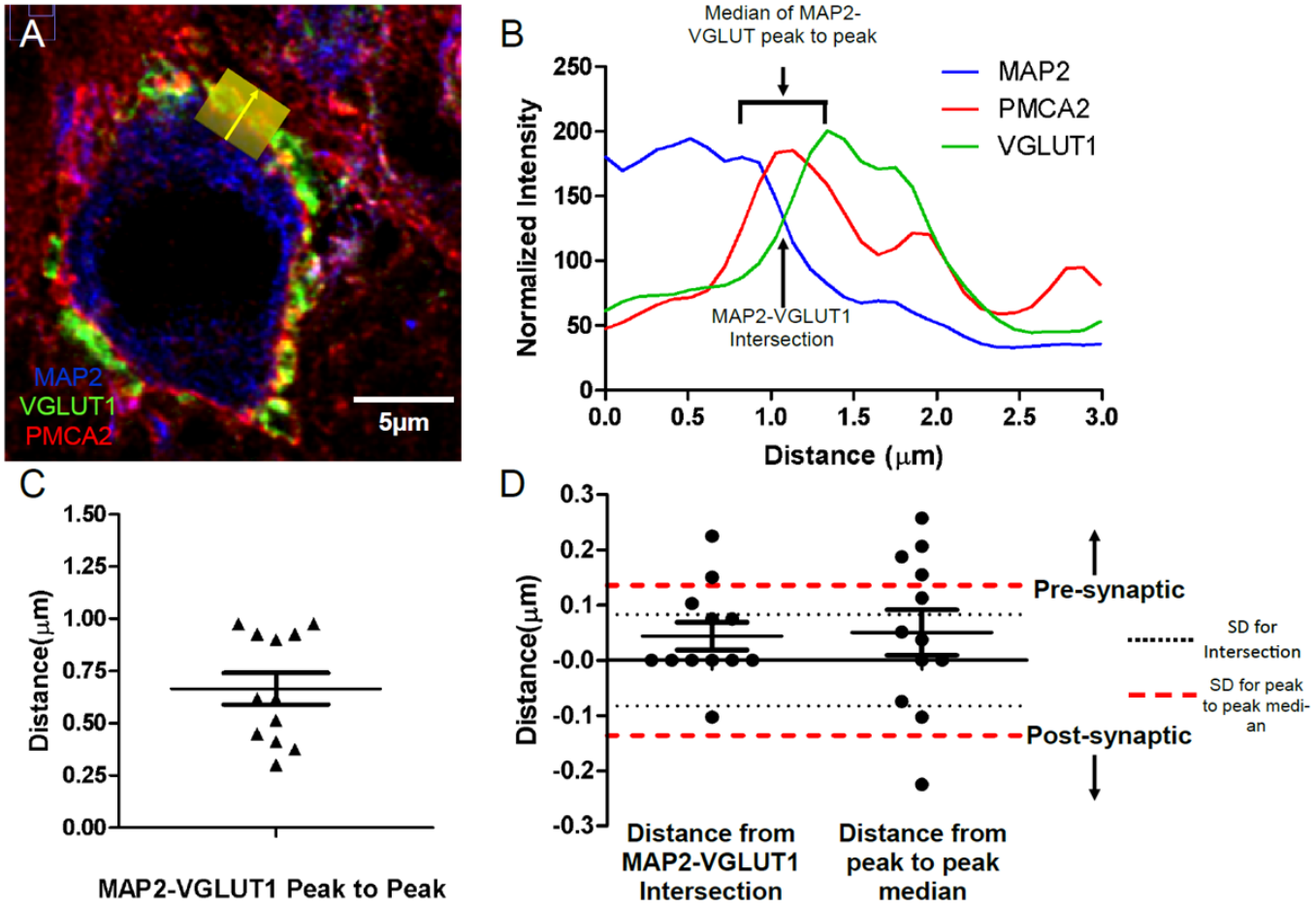


**Figure 2.4. Consecutive line scans suggest PMCA2 may be present on both pre– and post-synaptic membranes**. A) MNTB neurons were stained for VGLUT1 (green), a pre-synaptic marker, MAP2 (blue), a somatodendritic marker, and PMCA2 (red). B) The line scan from the yellow area depicted in A shows a separation between the post-synaptic marker (MAP2; blue) and the pre-synaptic marker (VGLUT1; green). PMCA2 (red) was intermediate between these two peaks in all line scans tested. C) The average distance between MAP2 and VGLUT1 was 666 nm (SEM=72nm). D) The average distance of the PMCA2 peak from the intersection was 43nm (SEM=24nm). The average distance of the PMCA2 peak from the median was 59nm (SEM=39nm). Both of these measures fell towards the pre-synaptic side but neither were more than one SD greater than zero (SD for intersection=black dotted line; SD for median=red dashed line). While the resolution of this method limits the conclusions drawn, it supports the possibility that PMCA2 is present on both the pre– and post-synaptic membranes.

## Chapter 3

## *dfw*$^{2J}$ mutants reveal a cell size gradient in the MNTB


### Summary

The medial nucleus of the trapezoid body (MNTB) is an auditory brainstem nuclei involved in sound localization. The specialized role of MNTB neurons requires fast and precise action potentials that must be accompanied by an efficient calcium clearance mechanism. The plasma membrane calcium ATPase 2 (PMCA2) may play a role in calcium clearance in MNTB neurons. *dfw*$^{2J}$ mutant mice have a null mutation in PMCA2 causing deafness in homozygotes (*dfw*$^{2J}$/*dfw*$^{2J}$) and high frequency hearing loss in heterozygotes (+/*dfw*$^{2J}$). When examining the gross morphology of MNTBs from *dfw*$^{2J}$ mutants we found no significant difference in MNTB volume or cell number suggesting PMCA2 is not required for MNTB neuron survival. There was a decrease in neuron size between wildtype and *dfw*$^{2J}$/*dfw*$^{2J}$.

The MNTB is organized along a tonotopic axis. MNTB neurons were divided into medial and lateral groups. In wildtype, medial cells were significantly smaller than the lateral cells suggesting the presence of a cell size gradient. This size gradient is decreased in +/*dfw*$^{2J}$ and absent in *dfw*$^{2J}$/*dfw*$^{2J}$. Diphtheria toxin receptor (DTR) mice in which hair cells have been

selectively eliminated show no gradient suggesting normal auditory activity is required for maintenance of the gradient. The size gradient in the MNTB of gerbil is abolished approximately 48 hours after hair cell activity is terminated by cochlear ablation or tetrodotoxin (TTX) treatment. The gradient returns in gerbils allowed to recover for 7 days after TTX treatment suggesting these changes in neuron size are plastic.

### 3.1 Introduction

One mechanism by which the mouse localizes sound is by calculating interaural intensity differences (IIDs). Sound transduction begins in the periphery where hair-cells transform sound from a mechanical signal to an electrochemical signal. This electrochemical signal is sent as an action potential to the superior olivary complex (SOC) in the auditory brainstem. This complex is responsible for comparing signals coming from each ear to calculate the IID (Figure 1.1; See von Gersdorff and Borst, 2002 for review). One of the nuclei in this complex is the MNTB. The MNTB receives inputs from the contralateral side and inverts this signal from excitatory to inhibitory so the signal can be compared to the excitatory signal coming from the ipsilateral side. Because the arrival times of these action potentials are being compared to calculate IIDs, MNTB neurons must fire precisely such that the temporal information is conserved throughout the circuit (Wang et al., 1998; Taschenberger and von Gersdorff, 2000). MNTB neurons must also be able to fire quickly. MNTB neurons have firing rates of more than 300 spikes per second *in vivo* (Kopp-Scheinpflug et al., 2008). To maintain precision and speed, residual calcium must be cleared to avoid either synaptic facilitation or depression therefore requiring an efficient calcium clearance mechanism. We hypothesize that PMCA2, the most efficient of the plasma calcium ATPases, plays an important role in this calcium clearance.

PMCA2 is a calcium ATPase that pumps calcium from inside the cell to the extracellular space. PMCA2 is localized in the stereocilia of hair cells and is required for hair cell survival (Dumont et al., 2001; Yamoah et al., 1998; Kozel et al., 1998; Kozel et al., 2002; McCullough and Tempel, 2004; Street et al., 1998; Takahashi et al.,1998; Yamoah et al., 1998). Spontaneous mutations have occurred in the gene that codes for PMCA decreasing PMCA2 expression and leading to hearing loss both in humans and mice (Schultz et al. 2005, McCullough et al. 2007, Brini et al. 2007, Ficarella et al. 2007). These mutations in mice provide a valuable genetic tool to study PMCA2 in a mammalian model. One example is the $dfw^{2J}$ mutation which is a frameshift mutation resulting in a premature stop codon (Street et al., 1998). $dfw^{2J}$ homozygous mutants ($dfw^{2J}/dfw^{2J}$) produce no PMCA2 protein causing deafness and ataxia while heterozygous mutants ($+/dfw^{2J}$) have high frequency hearing loss (McCullough and Tempel 2004). Another mutation that has occurred in mice is the *deafwaddler* mutation (*dfw*). This is a hypomorphic point mutation (Street et al., 1998) that renders the PMCA2 pump less efficient that wildtype. Calcium clearance studies suggest that *dfw/dfw* PMCA2 pumps at about 30% the efficiency as wildtype (Penheiter et al., 2001).

Since PMCA2 is necessary for normal haircell morphology and survival (Watson and Tempel, 2013), it is possible that PMCA2 is also required for normal MNTB neuron morphology. This study investigates if PMCA2 is required for MNTB neuronal survival. We show that PMCA2 is not necessary for neuronal survival and unexpectedly discover there is a cell size gradient in the MNTB which requires auditory inputs and PMCA2.

### 3.2 Methods

*Animals.* Adult (5-7 week old) CBA/CaJ deafwaddler (*dfw*$^{2J}$), CBA/CaJ deafwaddler (*dfw*) (Street et al., 1998), and B6 DTR (Tong et al., 2011; Gotlub et al., 2012) mice of either sex were obtained from the University of Washington Tempel Lab breeding colony. All manipulations were carried out in accordance with protocols approved by the University of Washington Animal Care Committee.

*Diphtheria toxin treatment.* Diphtheria toxin (DT) was administered to DTR mice genetically engineered to express the human diphtheria toxin receptor selectively in hair cells (Tong et al., 2011; Golub et al, 2012). A 50µg/Kg dose of DT (List Biological Laboratories, Inc. #150) was delivered via intramuscular injection to four week old DTR mice. By 6 days after DT injection, the DTR mice lose all of their hair cells and are completely deaf (Tong et al., 2011). After DT injection, DTR mice were allowed to survive for two weeks before tissue collection.

*Histology.* The animals were anesthetized with Nembutal and perfused with a saline-heparin solution followed by 4% paraformaldahyde. The brains were exposed in the skull and stored in 4% paraformaldahyde overnight. The brains were then dissected from the skull and post-fixed for an additional hour. The tissue was transferred to 10% sucrose in 0.1M phosphate buffer until sinking which took approximately 3 hours. The tissue was transferred again to 30% sucrose in 0.1M phosphate buffer where they remained until sinking, which took approximately 24 hours. Coronal sections 10 or 40 µm thick were cut through the brain stem using a freezing microtome. The free floating sections were stored in phosphate-buffered saline (PBS; pH 7.4).

*Nissl staining.* Alternating slices from each animal were mounted and stained in weak thionin for 5 minutes and then dehydrated using successively more concentrated baths of ethanol followed by successively more concentrated baths of xylene.

*Light microscopy.* Images for morphology experiments were taken with a Zeiss Axioplan 2ie using a 10x or 40x lens. Each section was positioned so that the midline was perpendicular or parallel to the x-axis of the image. The focal plane selected for these images was approximately in the center of the slice thickness to the nearest micron. For 10x images one image was taken. For 40x images 1-16 images were taken covering the entirety of the MNTB in that section. The 40x images were montaged together using MosaicJ in ImageJ.

*Neuron number.* To determine the number of neurons in each MNTB, all cells in the MNTB of stained sections were counted online using the optical dissector method (West et al., 1991). The slides were randomized to blind the counter to the genotype of the tissue. The cell counter focused up and down with a 40x lens in each square of a counting grid. Only those cells with a nucleus and nucleolous were counted. The total number of neurons present in each MNTB was estimated by multiplying by 2 since only half of the slices were analyzed (Figure 2A).

*MNTB volume.* The MNTB volume was determined using the cross sectional area of the MNTB in each thinion stained section. Images of the MNTB in each section were taken using a 10x lens and randomized for blind analysis. The MNTB was outlined using ImageJ, only cells that were darkly stained and less than 20μm from their nearest neighbor were included in the MNTB perimeter. This outline was used to calculate the area of the MNTB in each section. The volume of the MNTB was estimated by multiplying each MNTB area by 40μm, this value was doubled since only every other slice of the MNTB was analyzed. These individual areas were summed to find the total volume of each MNTB (Figure 2B).

*Neuron size.* Neuron size was measured using 40x montaged images. The montaged images were randomized for blind analysis. All cells in the image that contained a defined nucleus,

nucleolous, and unobstructed cell membrane were analyzed. The surface area as well as central x and y coordinates were recorded for each cell containing the defined criteria (Figure 2C).

*Tonotopic axis.* The tonotopic axis was defined as the longest line that could be drawn through the nucleus. This line was divided into thirds and lines were drawn perpendicular to the tonotopic axis to delineate medial, central, and lateral areas.

*Slice preparations.* Mice (P12–P16) were killed by decapitation in accordance with the UK Animals (Scientific Procedures) Act 1986 and brainstem slices containing the superior olivary complex (SOC) prepared as previously described (Johnston et al., 2008). Transverse slices (200 µm-thick) containing the MNTB were cut in a low-sodium artificial CSF (aCSF) at ~0°C. Slices were maintained in a normal aCSF at 37°C for 1 hr, after which they were stored at room temperature (~20°C) in a continually recycling slice-maintenance chamber. Composition of the normal aCSF was (mM): NaCl 125, KCl 2.5, $NaHCO_3$ 26, glucose 10, $NaH_2PO_4$ 1.25, sodium pyruvate 2, myo-inositol 3, $CaCl_2$ 2, $MgCl_2$ 1 and ascorbic acid 0.5; pH was 7.4, bubbled with 95% $O_2$, 5% $CO_2$. For the low-sodium aCSF, NaCl was replaced by 250 mM sucrose, and $CaCl_2$ and $MgCl_2$ concentrations were changed to 0.1 and 4 mM, respectively. Experiments were conducted at a temperature of $36^oC \pm 1$ using a Peltier driven environmental chamber (constructed by University of Leicester Mechanical and Electronic Joint Workshops) or using a CI7800 (Campden Instruments, UK) feedback temperature controller.

*Patch-clamp recording.* Whole-cell patch-clamp recordings were made from visually identified MNTB neurons (Nikon FN600 microscope with differential interference contrast optics) using a Multiclamp 700B amplifier (Molecular Devices, Sunnyvale, CA, USA) and pClamp-10 software (Molecular Devices), sampling at 50kHz and filtering at 10kHz. Patch pipettes were pulled from borosilicate glass capillaries (GC150F-7.5, OD: 1.5mm; Harvard

Apparatus, Edenbridge, UK) using a two-stage vertical puller (PC-10 Narishige, Tokyo, Japan). Their resistance was ~3.0 MΩ when filled with a patch solution containing (mM): KGluconate 97.5, KCl 32.5, HEPES 40, EGTA 5, $MgCl_2$ 1, $Na_2$phosphocreatine 5, pH was adjusted to 7.2 with KOH. Whole-cell series resistances were <10MΩ, compensated by 70% and recordings in which the series resistance changed more than 2MΩ were eliminated from analysis. All patch clamp recordings were done by Conny Kopp-Scheinpflug.

*Capacitance measures.* Cell capacitance was assessed in whole-cell voltage-clamp recordings using the pCLAMP-10 software. A -5mV pulse, which does not activate any voltage-dependent conductances were applied from a membrane potential of -60mV and 50 capacitive transients were recorded and averaged (Fig. 3.3). A logarithmic exponential fit was performed on the averaged transients and was used to find the time constant ($\tau$) of the decay. The steady state current was measured at 80% of the duration of the 10ms voltage pulse. The current difference ($\Delta I$) equals the voltage of the command step ($\Delta V$) divided by the sum of electrode resistance ($R_a$) and the input resistance ($R_i$). When calculating the charge under the transient, the settling time of the membrane voltage step is corrected by adding $\Delta I \times \tau$. The membrane capacitance is then derived from the following equation: $C_m=(Q_1+Q_2)/(\Delta V_m)$.

*Elimination of auditory activity in gerbil.* All experiments using gerbils were conducted using tissue collected by Pasic and Rubel 1989 or Pasic and Rubel 1991. These studies used adult Mongolion gerbils of either sex. Cochlear ablations were performed by removing the pinna, incising the tympanic membrane of one ear, and removing the malleus. The bony walls of all three turns of the cochlea were then opened, the cochlear contents were crushed and aspirated, and the modiolus was fractured. For TTX treatment, TTX crystals (Sigma Chemicals, St. Louis, MO) were suspended and placed on a disk. Small pieces of disk (0.1g) containing approximately

500ng of TTX were cut with a 17-gauge stub adapter. TTX blockade was obtained by removing the pinna, making an incision posterior to the ear canal, opening the mastoid bulla, and placing disk with TTX in the round window niche of the middle ear resting against the round window membrane. In animals receiving TTX treatment for 48 hours, the TTX was replaced after 24 hours to ensure adequate blockade. Animals in the group allowed to survive for 7 days after blockade had the disk containing TTX removed 20 or 44 hours after insertion. Previous experiments show that cell size of neurons in the cochlear nucleus are unaffected by placing polymer without TTX in the round window (Pasic and Rubel, 1989) and that blockade reliably lasts for 4 hours following removal of TTX (Pasic and Rubel, 1991). All treatment was unilateral and the contralateral MNTB was used for analysis. See Pasic and Rubel, 1989 and Pasic and Rubel, 1991 for complete methods.

*Statistics.* Data were analyzed using either a one way ANOVA and a Tukey post-hoc test or a paired t-test. A p value $< 0.05$ was considered significant. Error bars are SEM.

**3.3 Results**

*3.3.1 PMCA2 is not required for neuron survival*

To determine if PMCA2 is necessary for neuron survival in the neuron number (Figure 3.1A), MNTB volume (Figure 3.1B), and neuron size (Figure 3.1C) were quantified in Nissl stained sections from wildtype littermates, +/$dfw^{2J}$, and $dfw^{2J}/dfw^{2J}$ mice. There was no significant difference in neuron number (Figure 3.1A; F=0.1310; p=0.8797) or MNTB volume (Figure 3.1B; F=1.965; p=0.4508) via a one-way ANOVA between the genotypes. Neuron number was not calculated for *dfw/dfw* because there was no difference in $dfw^{2J}/dfw^{2J}$, which have a more severe phenotype.

*3.3.2 A cell size gradient discovered in wildtype mice is absent in deafwaddler mutants*

Neurons were significantly smaller in $dfw^{2J}/dfw^{2J}$ than wildtype in a one-way ANOVA and Tukey post-hoc test (Figure 3.1C; F=5.894; p=0.04). To determine if these changes in cell size occurred differentially along the tonotopic axis, the nucleus was divided into thirds and cells were assigned to medial, central, or lateral groups (Figure 3.2A). We tested animals with varying PMCA2 function from wildtype which have 100% function, $+/dfw^{2J}$ with about 60% function, *dfw*/*dfw* with approximately 30% function, and $dfw^{2J}/dfw^{2J}$ which have 0% function (Table 1). In wildtype animals, the medial cells were significantly smaller than the lateral cells (Figure 3.2B; p=0.02). In $+/dfw^{2J}$, the difference in cell size was decreased and no longer significant (Figure 3.2B; p=0.08). In *dfw*/*dfw* the difference had decreased even more while in $dfw^{2J}/dfw^{2J}$ mice medial and lateral cells were the same size (Figure 3.2B). Figure 3.2C shows the difference in medial and lateral cells for each individual mouse. Figure 3.2D shows a scatter plot of the individual neurons from one wildtype MNTB and one $dfw^{2J}/dfw^{2J}$ MNTB. The linear regression for cells in wildtype mice is significantly non-zero (Figure 3.2D; p=0.01) but is not significant in $dfw^{2J}/dfw^{2J}$ demonstrating that there is a cell size gradient in wildtype which is absent in $dfw^{2J}/dfw^{2J}$.

*3.3.3 Capacitance recapitulates the presence of a cell size gradient in wildtype which is absent in $dfw^{2J}$ mutants*

Capacitance of the membrane ($C_m$) is a measurement of the ability of the membrane to build up and store charge. $C_m$ is directly related to the surface area of the membrane of a cell. Larger cells have more membrane and therefore more capacitance than smaller cells. As a separate measure of cell membrane surface area, we took capacitance measurements in wildtype, $+/dfw^{2}$,

and *dfw*$^{2J}$/*dfw*$^{2J}$. The capacitance data corroborated the cell sizing data in that medial neurons had significantly lower capacitance than lateral cells in wildtype animals in a paired t-test (Figure 3.2A: p=0.001). This difference in capacitance was reduced although still significant in +/*dfw*$^{2}$ (Figure 3.2A; p=0.024), and was completely gone in *dfw*$^{2J}$/*dfw*$^{2J}$. The linear regression for wildtype neurons is significantly non zero (Figure 3.3B; p=0.0001), but is not significant for *dfw*$^{2J}$/*dfw*$^{2J}$ neurons. The difference between tau in medial and lateral cells is significant in wildtype neurons (p=0.007) but not in +/*dfw*$^{2J}$ or *dfw*$^{2J}$/*dfw*$^{2J}$ neurons.

*3.3.4 Auditory activity is necessary to maintain the cell size gradient in the MNTB*

The PMCA2 mutant mice we tested lack PMCA2 in the MNTB but these mice also have hearing loss. To determine if the elimination of cochlear activity could cause a change in the cell size gradient, we selectively abolished hair cells in DTR mice (Table 1). These mice showed no significant difference in cell size between medial and lateral cells in a paired t-test suggesting that auditory inputs are necessary to maintain the cell size gradient in the MNTB (Figure 3.2B,C).

*3.3.5 A size gradient present in the MNTB of gerbil requires auditory activity*

Mice hear in a higher frequency range than humans. To determine if the cell size gradient generalized to a mammal that hears in the lower frequency range we looked at the MNTB of gerbil. We found that medial cells are significantly smaller than lateral cells in gerbils in a paired t-test (Figure 3.4; p=0.0004). To determine if cochlear activity is necessary to maintain the cell size gradient in the MNTB, we looked at tissue from gerbils either 24 or 48 hours after cochlear ablation. Twenty four hours after cochlear ablation, the difference in size between

medial and lateral cells was still significant (Figure 3.4A; p=0.01), but 48 hours after cochlear ablation, the difference was no longer significant suggesting 48 hours is sufficient for the cell size gradient to be abolished (Figure 3.4). To determine if the cell size gradient could return after a period of depravation, TTX was inserted into the round window to block action potentials arising in the cochlea. TTX is a sodium channel blocker that prevents action potentials from propagating in the spiral ganglion cells and therefore eliminating sound driven activity. After 24 hours of TTX treatment, the size difference between medial and lateral cells was no longer significant and by 48 hours, the cell size was indistinguishable between medial and lateral cells (Figure 3.4). Figure 3.4B shows the average cell size for medial, central, and lateral cells for each individual gerbil tested.

*3.3.6 The cell size gradient recovers when activity is restored after a period of deprivation*

TTX temporarily blocks activity but is reversible. After TTX is removed the hair cells recover and activity resumes. In gerbils allowed to recover from 48 hours of TTX treatment for 7 days, the size gradient returned and medial cells were again significantly smaller than lateral cells in a paired t-test (Figure 3.4; p=0.02).

## 3.4 Discussion

Tonotopic gradients exist throughout the auditory system. Tonotopic organization is established in the cochlea where hair cells are arranged based on the best frequency to which they respond. This organization is carried on through the auditory brainstem and all the way to the auditory cortex. To date, we are aware of tonotopic gradients in cell morphology and size as well as gradients involving ion channels and receptors. The hair cells in the cochlea show differences in

stereocilia length and somata size. Those cells responding best to low frequencies have longer stereocilia and larger somata while those responding to high frequencies have shorter stereocilia and smaller somata (Corwin and Warchol, 1991; Ashmore and Gale, 2000). In the spiral ganglia there is a tonotopic arrangement of synaptic proteins where there is more α-GluR2/3 in neurons responding to high frequencies than in neurons responding to low frequencies (Flores-Otero and Davis, 2011). In MNTB there are a variety of ion channel gradients along the tonotopic axis. For example, Kv3.1 increases lateral to medial (von Hehn et al., 2004) while Kv1.3 increases medial to lateral in the MNTB (Leao et al., 2006).

These tonotopic gradients are features of the auditory system essential for each cell to perform its specialized task and are characteristics unique to auditory nuclei. In this study we have defined a cell size gradient in the MNTB dependent on auditory activity. As summarized in Figure 3.5, four independent approaches were employed to demonstrate that maintenance of the gradient requires auditory inputs. Two of these approaches utilized mouse mutants while the other utilized surgical and pharmacological manipulation of the cochlea in gerbils. The TTX treatment in gerbils provided a tool to show that the neuron size gradient in the MNTB is able to recover after a period of deprivation.

While two previous publications noted a difference in MNTB cell size (Pasic et al., 1991), to our knowledge, this is the first systematic characterization of the cell size gradient along the tonotopic axis. This finding was not only demonstrated using histology, but also with capacitance readings which may give us some insight into how these gradients may affect the physiological behavior of these neurons.

Capacitance of the membrane ($C_m$) is a measurement of the ability of the membrane to build up and store charge. $C_m$ is directly related to the surface area of the membrane of a cell.

Larger cells have more membrane and therefore more capacitance than smaller cells. Capacitance affects the amount of time it takes for a cell to reach any particular voltage. The more charge that is able to build up on the membrane, the longer it will to take to reach peak voltage in the cell body. This phenomenon can be explained by the equation: $\tau = R_m C_m$. Where $\tau$ is the time constant and $R_m$ equals the resistance of the membrane. If $C_m$ increases $\tau$ will also increase given the resistance remains constant. For this reason, smaller cells are able to fire more rapidly than large cells. The cell size gradient in the MNTB suggests that medial cells, which are smaller than lateral cells, should be able to fire more quickly than the larger lateral cells. Indeed, *in vivo* recordings show that medial cells responding best to high frequencies fire more quickly than cells responding to low frequencies (Sonntag et al, 2009). Adjusting cell size may be a way for neurons to calibrate themselves to fire at specific rates. Conversely, cell size may be affected by firing rate and medial cells are smaller *because* they fire rapidly.

Data presented here show that auditory activity is required to maintain the cell size gradient. Cochlear activity was manipulated using four different methods in two different animal models. In mice, hair cell activity was eliminated using PMCA2 mutants and mice genetically engineered for hair cell abolition with DT injection. In gerbil, hair cell activity was eliminated through cochlear ablation or TTX treatment. The cell size gradient was absent in all animals in which cochlear activity was eliminated.

Additionally, the cell size gradient was able to recover after a period of deprivation. Gerbils treated with TTX for 48 hours show a dramatic decrease in cell size and the abolition of the cell size gradient. However, animals allowed to recover for 7 days after TTX treatment show a significant difference in cell size between medial and lateral cells indicating that the gradient has returned. This suggests that this phenomenon is not simply determined during development

but neurons are able to adjust their size in the adult brain. The recovery of the gradient shows changes in cell size are not a permanent but are plastic and adjustable according to the auditory inputs available.

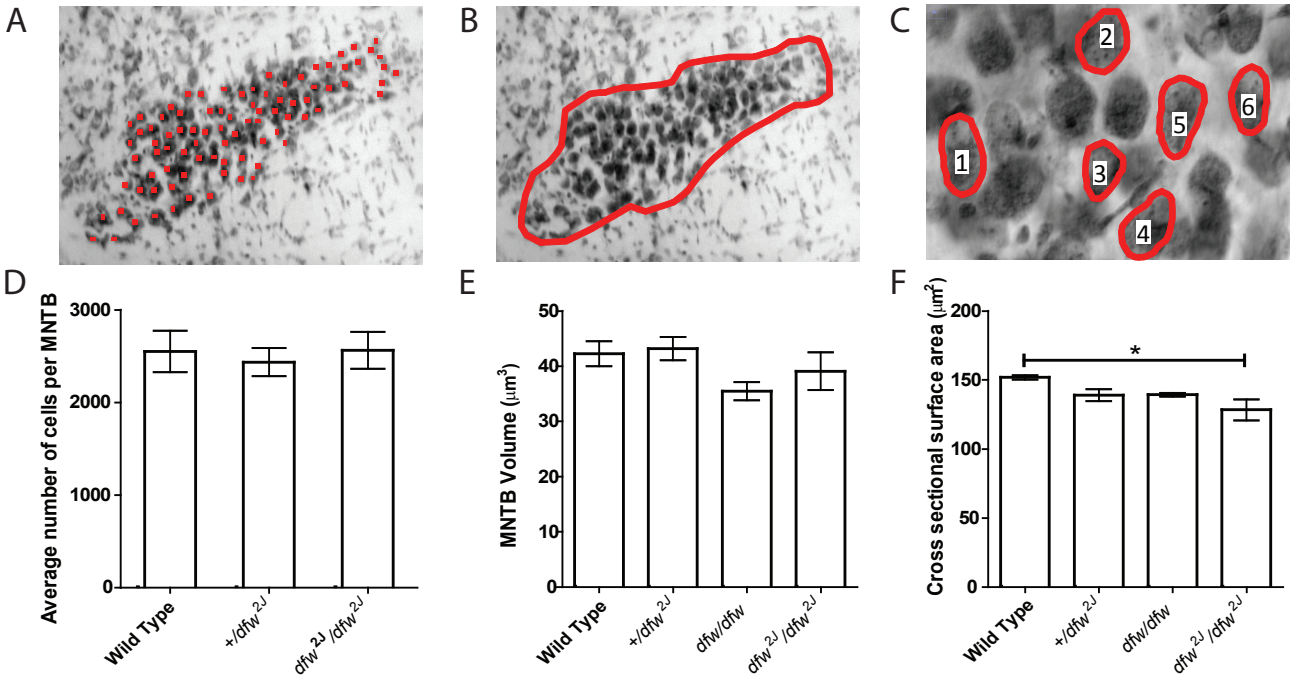


**Figure 3.1. MNTB Morphology is similar in wildtype and *dfw$^{2J}$* mutants.** Nissl stained coronal sections were used to estimate A) cell number, B) MNTB volume, and C) average cell size in wildtype, +/*dfw2J*, and *dfw$^{2J}$*/*dfw$^{2J}$* mutants. D) There was no significant difference in cell number between any of the genotypes via one-way ANOVA (n=3 mice per group). E) There was no significant difference in MNTB volume between any of the genotypes via one-way ANOVA (n=6 MNTB per group). F) There was a significant decrease in the average cross sectional area between wildtype and *dfw$^{2J}$*/*dfw$^{2J}$* mutants via one-way ANOVA and Tukey post-hoc analysis (*p≤0.05, n=1854 cells from 9 mice). Error bars=SEM.

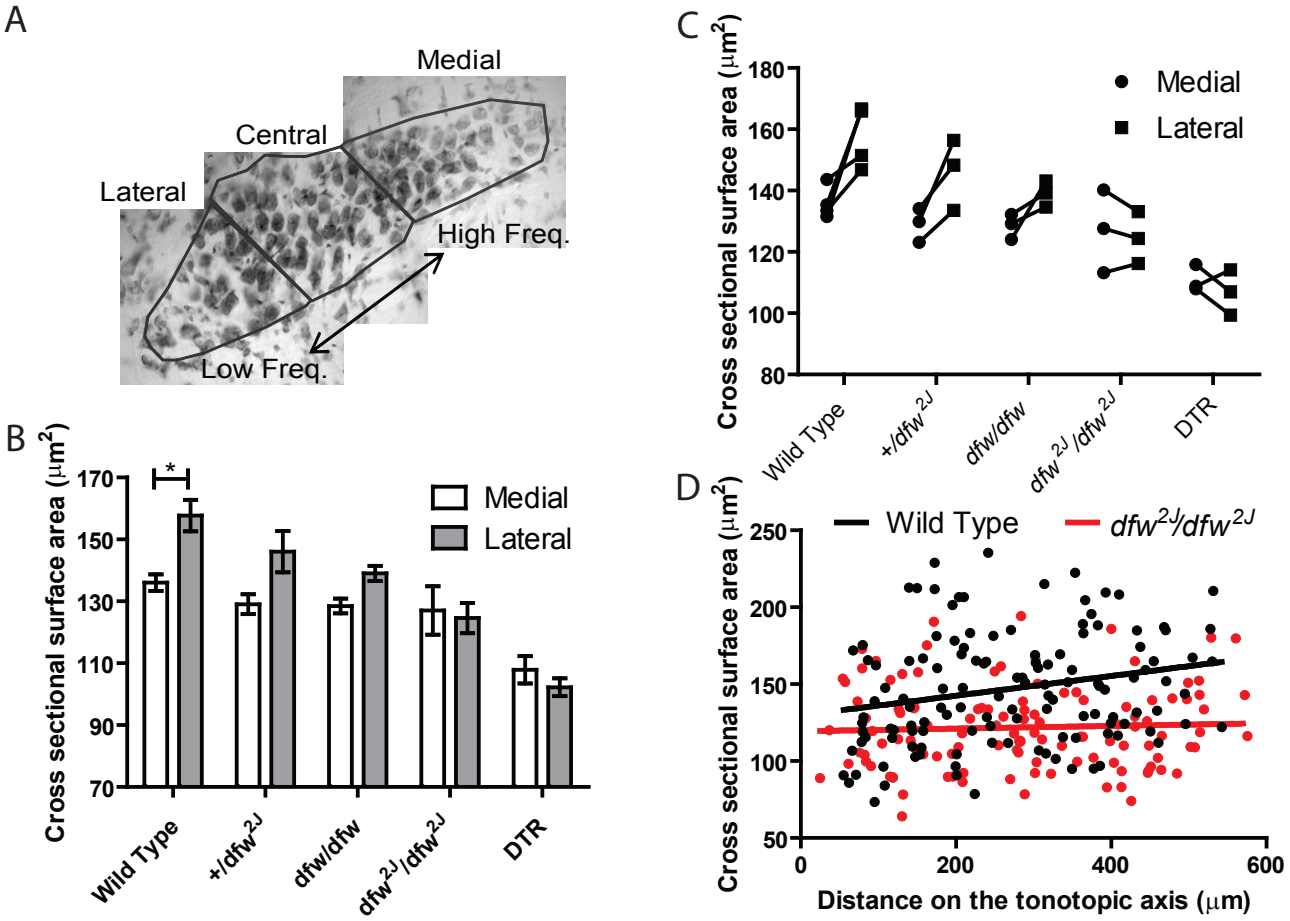


**Figure 3.2. Cell size gradient in the mouse MNTB.** Nissl stained coronal sections were used to estimate average cell size in wildtype, +/*dfw*$^{2J}$, *dfw*/*dfw*, *dfw*$^{2J}$/*dfw*$^{2J}$, and DTR mice. Cell size was determined using ImageJ to calculate cross sectional area. A) Cells were defined as medial if located in the medial third of the MNTB or lateral if located in the lateral third of the MNTB. B) There was a significant increase in the size of lateral cells as compared to medial cells in the wildtype animals via a paired t-test ($p<0.0001$). There was no significant increase in the size of lateral cells in the +/*dfw*$^{2J}$, *dfw*/*dfw*, *dfw*$^{2J}$/*dfw*$^{2J}$, or DTR mice. Error bars are SEM. C) Individual average cell size for medial and lateral cells in each MNTB. D) Scatter plot of location along the tonotopic axis vs. cross sectional surface area for one MNTB from a wildtype and *dfw*$^{2J}$/*dfw*$^{2J}$. The linear regression is significantly different from zero for wildtype ($p=0.01$) but not for *dfw*$^{2J}$/*dfw*$^{2J}$.

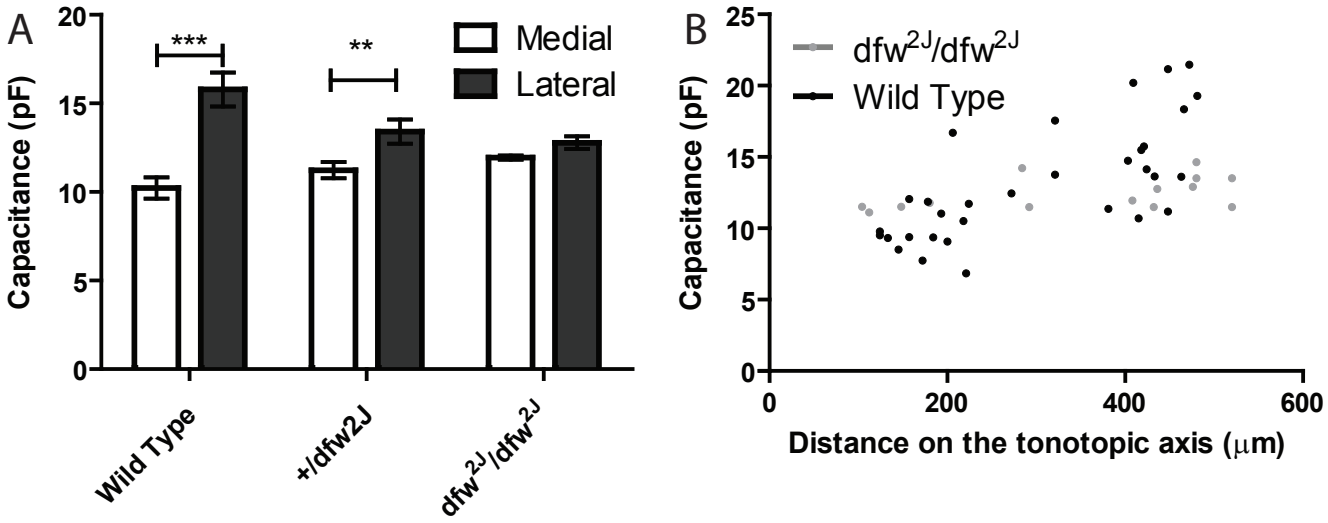


**Figure 3.3. A capacitance gradient is present in wildtype but is decreased in *dfw$^{2J}$* mutants.** A) Capacitance measurements corroborate histology data showing lateral cells are significantly larger than medial cells in wildtype via a paired t-test ($p \leq 0.001$) and +/*dfw$^{2}$* ($p=0.02$) but there is no significant difference between cells in *dfw$^{2J}$*/*dfw$^{2J}$* mutants. Error bars are SEM. B) Scatter plot of capacitance vs. position on the tonotopic axis for wildtype and *dfw$^{2J}$*/*dfw$^{2J}$*.

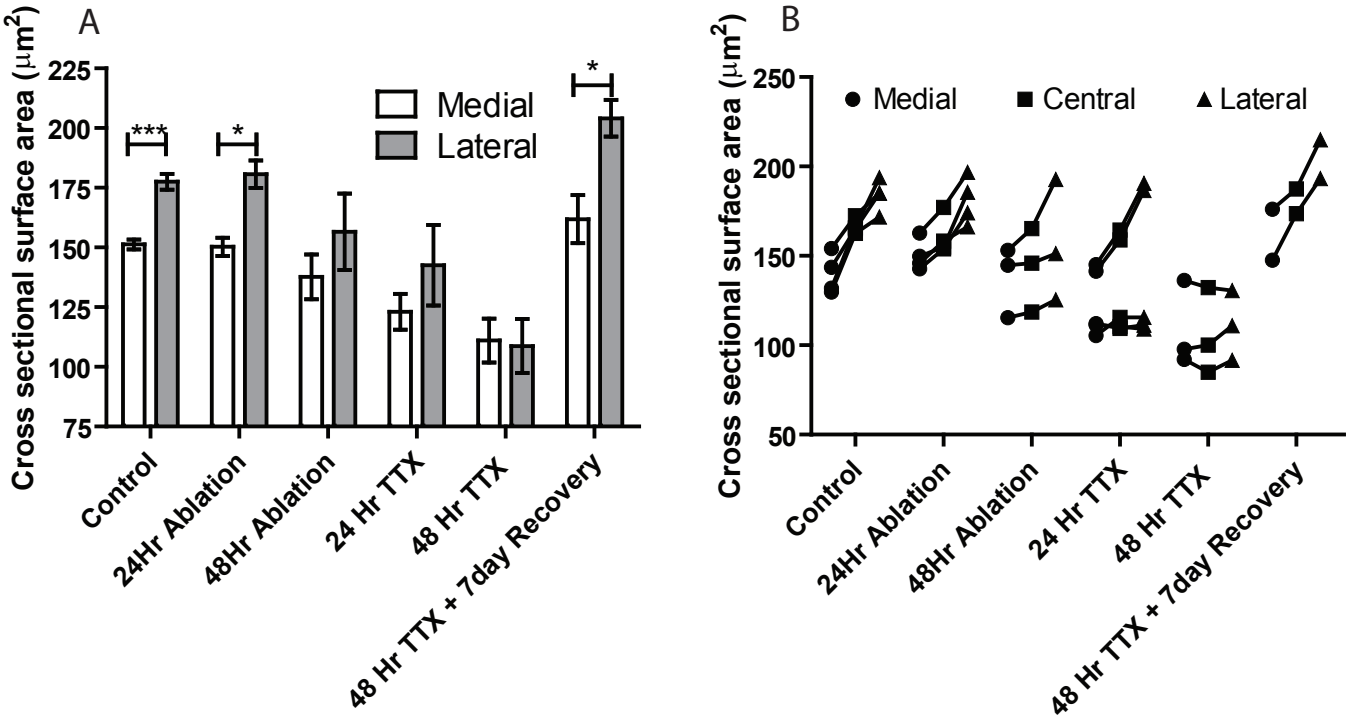


**Figure 3.4. Cell size gradient in the gerbil MNTB.** Nissl stained coronal sections were used to estimate average cell size in adult gerbils. Some animals had cochlear ablations and tissue was collected either 24 hours or 48 hours post surgery. Other subjects had TTX treatment for 24 or 48 hours and tissue was collected either immediately following TTX treatment, or 7 days after TTX treatment. A) Control gerbils showed a cell size gradient as did subjects with tissue collected 24 hours after cochlear ablation (paired t-test; p=0.0004 and p=0.01 respectively). Tissue collected 48 hours after cochlear ablation showed a diminished gradient. Gerbils treated with TTX for 24 or 48 hours showed a decreased or no cell size gradient, but in those animals allowed to recover for 7 days, the gradient had returned (paired t-test; p=0.02). Error bars are SEM. B) Individual average cell size for medial, central and lateral regions of each MNTB.

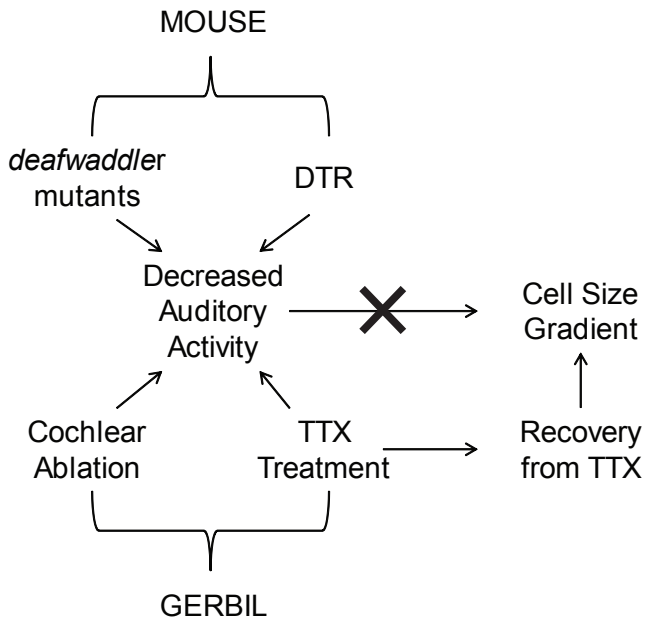


**Figure 3.5. Auditory activity is required to maintain the cell size gradient in mice and gerbils**. Normal hearing mice and gerbils both show a cell size gradient. If auditory activity is eliminated through a genetic mutation, DT treatment, cochlear ablation, or TTX treatment the cell size gradient is absent. If auditory activity returns after a period of deprivation the cell size gradient returns.

## Chapter 4

## Homogenous expression of PMCA2 across the tonotopic axis is not affected by auditory activity

### Summary

The medial nucleus of the trapezoid body (MNTB) is arranged tonotopically with lateral cell responding best to low frequencies and medial cells responding best to high frequencies (Sonntag et al., 2009). There are gradients of ion channels along this tonotopic axis in the MNTB that require auditory activity (Li et al., 2001, von Hehn et al., 2004; Leao et al,. 2006; Gazula et al, 2010; Strumbos et al., 2010) (Figure 1.3). We used immunocytochemistry (ICC) to determine if plasma membrane calcium ATPase 2 (PMCA2) is expressed homogenously throughout the mouse MNTB. While total PMCA2 is greater in lateral cells than in medial cells, this correlates to a cell size gradient in the MNTB where lateral cells are larger and medial cells are smaller. When controlling for differences in cell size by calculating average optical density, the difference between lateral and medial cells disappears suggesting the density of PMCA2 is homogenous along the tonotopic axis.

Ion channel gradients in the MNTB are disrupted in deaf mice models (von Hehn et al., 2004; Leao et al., 2006: Strumbos et al., 2010). To determine if auditory inputs affect PMCA2 expression we used diphtheria toxin receptor (DTR) mice as a deaf mouse model. DTR mice have been genetically engineered to selectively express the human diphtheria toxin receptor in hair cells such that a sub-lethal dose of diphtheria toxin (DT) selectively ablates hair cells (Tong et al., 2011; Golub et al., 2012). Two weeks after DT injection, DTR mice show no gradient in total or average optical density suggesting that PMCA2 is homogenously expressed in mice lacking auditory activity. There was no significant difference in average optical density between controls and DT injected DTR mice suggesting auditory activity does not affect the density of PMCA2 in the MNTB. This finding solicits questions as to whether total protein or protein density is most important for neuron function.

### 4.1 Introduction

The MNTB has been used as a model for studying synaptic plasticity so knowing what ion channels and receptors are present is essential for creating a complete understanding of how these neurons work. The membrane composition of MNTB neurons is complex. Throughout development, the morphology, ion channel composition, and receptor expression changes. This requires researchers to take age in to consideration when compiling data from different studies. Adding to the complexity, several studies have found ion channels that are expressed differentially along the tonotopic axis of the MNTB (Figure 1.3A). These ion channel gradients have also been shown to be abolished when auditory activity is absent (Li et al., 2001, von Hehn et al., 2004; Leao et al,. 2006; Gazula et al, 2010; Strumbos et al., 2010) (Figure 1.3B). These studies suggest that MNTB neurons may be able to subtly change their firing properties by

changing ion channel composition based on stimulation and requires researchers to control for best frequency as well as auditory inputs when comparing neurons.

In chapter 1 we showed that PMCA2 is highly expressed in the MNTB and likely plays a role in clearing calcium both from the pre- and post-synaptic sides of the synapse. Although PMCA2 is not an ion channel, it is important for regulating ion channel concentrations. For this reason, we hypothesized that PMCA2 may also be expressed in a gradient along the tonotopic axis of the MNTB. We also hypothesized that PMCA2 expression could be affected by auditory inputs. Either the total amount of PMCA2 may be adjusted or the pattern of expression may be altered based on auditory stimulation. To test this hypothesis, we used the DTR mouse which have been genetically engineered to selectively express the diphtheria toxin receptor in hair cells. This allows us to selectively ablate hair cells in the cochlea with a sublethal injection of DT (Golub et al., 2012). In previous studies a variety of mouse models have been used to abolish these gradients including age related hearing loss in BL/6 (Li et al., 2001), the congenitally deaf *dn/dn* mouse (Leao et al., 2006) and the *fmrp/fmrp* mouse (Strumbos et al., 2010).

The DTR mouse is arguably a cleaner way of eliminating auditory activity because this mouse model allows the auditory system to develop normally in contrast to deaf mouse models that have congenital hearing loss (*dn/dn; fmrp/fmrp*). Hair cells are then eliminated at a discrete time point in contrast to a slow deterioration that occurs in age related hearing loss (BL/6). We were also able to use $dfw^{2J}$ mice which express about 60% PMCA2 protein compared to wildtype (Watson and Tempel, 2013) to validate our method.

**4.2 Methods**

*Animals.* Adult (5-7 week old) CBA/CaJ deafwaddler (*dfw*$^{2J}$), , and DTR (Tong et al., 2011; Gotlub et al., 2012) mice of either sex were obtained from the University of Washington Tempel Lab breeding colony. All manipulations were carried out in accordance with protocols approved by the University of Washington Animal Care Committee.

*Histology.* The animals were anesthetized with Nembutal and perfused with a saline-heparin solution followed by 4% paraformaldahyde. The brains were exposed in the skull and stored in 4% paraformaldahyde overnight. The brains were then dissected from the skull and post-fixed for an additional hour. The tissue was transferred to 10% sucrose in 0.1M phosphate buffer until sinking which took approximately 3 hours. The tissue was transferred again to 30% sucrose in 0.1M phosphate buffer where they remained until sinking, which took approximately 24 hours. Coronal sections 10 or 40 μm thick were cut through the brain stem using a freezing microtome. The free floating sections were stored in phosphate-buffered saline (PBS; pH 7.4).

*Immunocytochemistry.* Tissue from one control mouse, either a wildtype litter mate or uninjected DTR mouse, was processed simultaneously with each +/dfw$^{2J}$ and DT injected DTR mouse respectively. The fixed floating sections were treated with primary antibody for PMCA2 at a dilution of 1:250 in PBS with 0.3% Triton X-100 for 2 hours at room temperature. The sections were washed in PBS overnight at 4°C. The sections were then incubated with microtubule associated protein 2 (MAP2) primary antibody at 1:1000 in PBS with 0.3% Triton X-100 for 1.5 hours at room temperature. The sections were washed in PBS before incubating in AlexaFlour secondary antibodies (1:200; Molecular Probes, Eugene, OR) for 2 hours at room temperature.

*Primary Antibodies.* Polyclonal anti-PMCA2 (catalog No. PA1-915) made in rabbit was purchased from Affinity Bioreagents (Golden, CO). The immunogen is a synthetic peptide

corresponding to amino acid residues 5-19 of human PMCA2 protein. The sequence of the immunogen is TNSDFYSKNQRNESS. This sequence is completely conserved between human and mouse PMCA2. Monoclonal anti-MAP2 (catalog No. MAB3418) made in mouse was purchased from Chemicon International. The immunogen is bovine brain microtubule protein. The antibody binds specifically to MAP2a and MAP2b.

*Microscopy.* Images were taken with a Zeiss Axiovert microscope using a 40x objective. Montages of each MNTB were made using Sclidebook. A 7μm thick z-stack of each montage was deconvolved using the Huygens deconvolution system and the middle image was extracted for analysis.

*Diphtheria toxin treatment.* DT was administered to DTR mice which are genetically engineered to express the human diphtheria toxin receptor selectively in hair cells (Tong et al., 2011; Golub et al, 2012). A 50μg/Kg dose of DT (List Biological Laboratories, Inc. #150) was delivered via intramuscular injection to four week old DTR mice. By 6 days after DT injection, the DTR mice lose all of their hair cells and are completely deaf (Tong et al., 2011). After DT injection, DTR mice were allowed to survive for two weeks before tissue collection.

*Auditory Testing.* Auditory brainstem responses were taken for DTR mice and controls before the tissue was processed to verify that DT injected mice were deaf and control mice could hear. The auditory brainstem response was recorded by two electrodes placed subcutaneously over the forebrain and brainstem. Frequencies tested ranged from 5.6kHz to 40kHz. Tones were 3ms long with a 1ms rise/fall $\cos^2$ function (delivered with alternating polarity). Threshold was defined as the frequency at which there was a recognizable wave for at least 2 out of 3 trials.

*Image Processing.* Images were randomized to blind the observer selecting the regions of interest (ROIs). ROIs were drawn around cells in MAP2 images with a nucleus and defined cell

membrane (Figure 4.1A). This ROI was used to collect cross sectional surface area. Since MAP2 only stains the principal cell, each ROI was enlarged by 1μm to include the calyx of Held. (Figure 4.1B). The smaller ROI was subtracted from the larger ROI to create an ROI that attempts to select the membrane area of each cell. These membrane ROIs were transferred to the PMCA2 image. Raw intensity of each pixel from the PMCA2 channel was collected. Average intensity was calculated by adding the raw intensities and dividing by the number of pixels in each ROI. (Figure 4.1C). Intensities were either normalized to the average intensity of the control for that group (Figure 4.2) because the comparison was being made between subjects, or to the brightest pixel in that MNTB (Figures 4.4 and 4.5) because comparisons were made within subjects. Each MNTB was divided into thirds and cells were grouped into lateral, central, or medial groups based on their location (Figure 4.1D).

## 4.3 Results

### *4.3.1 Auditory activity does not affect the total amount of PMCA2 in the MNTB*

To determine if auditory activity affects PMCA2 expression in the MNTB we compared expression between DT injected DTR mice and uninjected controls. DT injected mice were tested by ABR before tissue collection to verify they were deaf. All DT mice showed no detectable thresholds as compared to uninjected controls which showed normal thresholds. PMCA2 integrated intensity (total PMCA2) was calculated for the 1μm thick border surrounding MAP2 cell body labeling. There was no difference in total PMCA2 expression between deaf mice and controls suggesting auditory activity does not affect the expression of PMCA2 in the MNTB (Figure 4.2).

*4.3.2 MAP2 labeling verifies a cell size gradient in the MNTB*

Cross-sectional surface area was calculated using ROIs selected from MAP2 images (Figure 4.1A). There was a medial to lateral cell size gradient in hearing controls that was absent in deaf mice reaffirming that auditory activity is required to maintain the cell size gradient in the MNTB (Figure 4.3)

*4.3.3 Analysis of +/dfw$^{2J}$ mice validates method*

To verify that our method was able to detect a change in PCMA2 expression we analyzed MNTBs from +/dfw$^{2J}$ mice. These mice expressed about 60% total PMCA2 compared to wildtype (Watson and Tempel, 2013). Using this method we were able to detect about a 40% decrease of PMCA2 in +/dfw$^{2J}$ compared to controls verifying that our method works (Figure 4.2).

*4.3.3 PMCA2 density is homogenous throughout the MNTB while total PMCA2 increases with cell size*

PMCA2 integrated intensity (total PMCA2) or average integrated intensity (PMCA2 density) was calculated for the 1µm thick border surrounding MAP2 cell body labeling. Cells were divided into medial, central, or lateral groups based on their location along the tonotopic axis in the MNTB (Figure 4.1D). Control mice showed a gradient of total PMCA2 expression (Figure 4.4). This increase in total PMCA2 trended in the same direction as the increase in cell size. When controlling for the change in cell size by calculating average PMCA2 expression, the data showed PMCA2 density was homogenous throughout the MNTB (Figure 4.5).

*4.3.4 Auditory activity does not change PMCA2 density in the MNTB*

DT injected DTR mice lacked a gradient of total PMCA2 along the tonotopic axis as compared to uninjected controls which did show a gradient. This occurred because DT injected DTR mice also lacked a cell size gradient. When controlling for cell size by calculating average PMCA2 expression, the data showed there was no difference in PMCA2 density between DT injected DTR mice and uninjected controls (Figure 4.5).

## 4.4 Discussion

Previous studies have shown ion channel expression is disrupted by eliminating auditory activity (Figure 1.2). PMCA2 is not an ion channel, but it is involved in controlling ion concentrations so we hypothesized that it may be expressed in a gradient as well. It would make sense that with decreased stimulation, there would be a decreased influx of calcium and thus a decreased need for PMCA2 to clear calcium. While ICC is notorious for not being quantitative, we developed a method to measure PMCA2 expression using ICC and verified our method was able to detect a decrease in PMCA2 by showing there was a 40% decrease in total PMCA2 expression in +/dfw$^{2J}$ mice as expected (Figure 4.2). We also showed that using MAP2 to select ROIs could detect a cell size gradient in cross sectional surface area as described in Chapter 3 (Figure 4.3). These data validate that this method is sufficient to comparatively study patterns of PCMA2 expression.

We did not see a decrease in total PMCA2 expression in deaf mice as compared to their hearing controls. This is interesting because the neurons in deaf mice are not firing nearly as much as they are in deaf controls if at all, yet they still produce PMCA2 at the same rate. This indicates that PMCA2 expression does not seem to be regulated by activity or the increases in

calcium concentration that come with a high level of stimulation. There must be some other mechanism regulating PMCA2 expression that is independent of activity.

Next we showed that there is a gradient of total PMCA2 expression along the tonotopic axis in control mice that corresponds to the gradient in cell size along the tonotopic axis. Both gradients are absent in deaf mice. When controlling for cell size by calculating PMCA2 density, there is no gradient in either hearing controls or deaf mice. This indicates that while there is a gradient in total PMCA2 in control mice, this is due to the fact that the cell size increases along the tonotopic axis. More PMCA2 must be made to maintain the same PMCA2 density in the membrane in larger cells. This suggests that PMCA2 density may be more important in regulating calcium concentrations rather than the total amount of PMCA2 in the membrane.

In summary, there is a gradient of total PMCA2 protein in control mice that correlates with the cell size gradient. PMCA2 density, however, is homogenous throughout the MNTB. Auditory activity does not appear to effect PMCA2 expression in the MNTB.

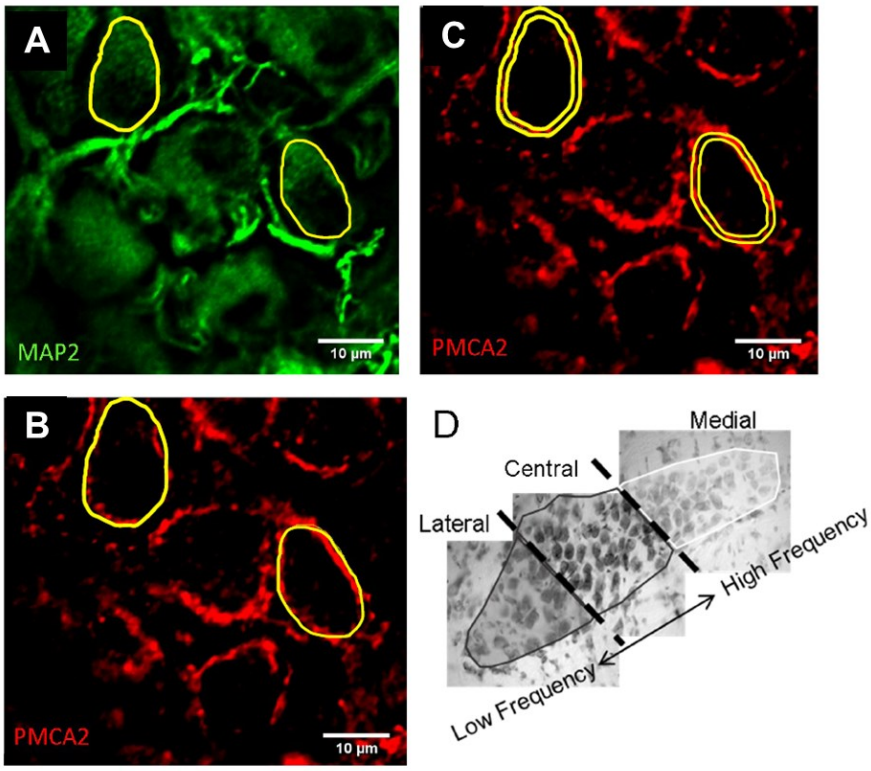


**Figure 4.1 Methods for PMCA2 gradient**. Tissue from adult control mice and deaf (DTR) mice were processed simultaneously. Images were taken using a 40x lens on a Zeiss Axiovert microscope. Images were montaged together using Slidebook 5 and deconvolved using the Huygens deconvolusion system. Images were randomized to blind the observer selecting the regions of interest (ROIs). (A) ROIs were drawn around cells in MAP2 images with a nucleus and defined cell membrane. This area was used to calculate cross sectional surface area. (B) ROIs were transferred to the PMCA2 image. Since MAP2 only stains the principal cell, each ROI was enlarged by 1µm to include the Calyx of Held. (C) The smaller ROI was subtracted from the larger ROI to calculate raw intensity, and average intensity from the PMCA2 images.

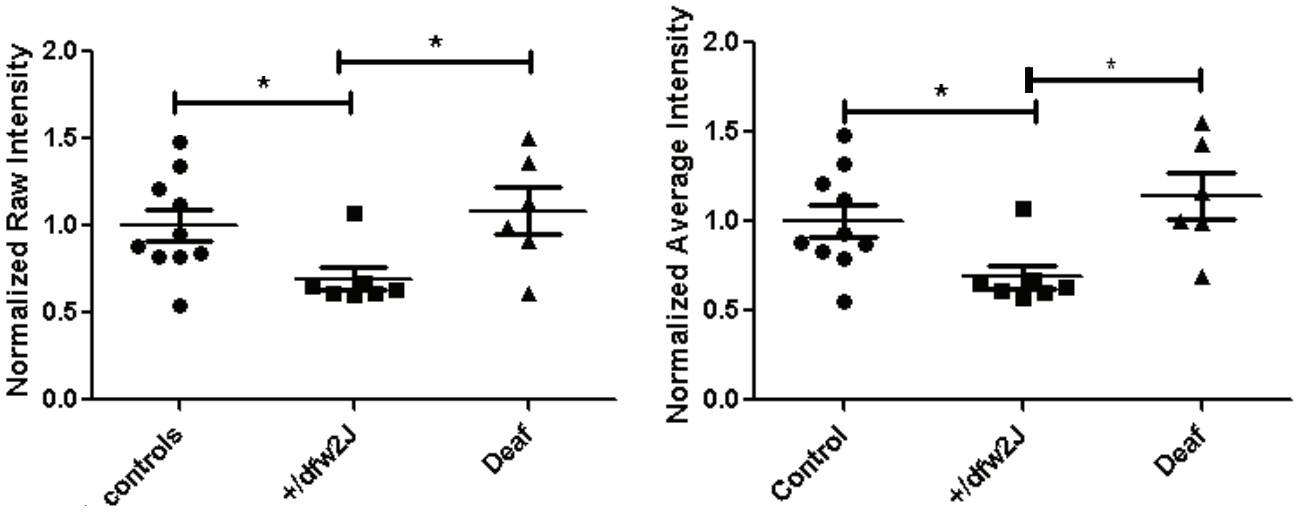


**Figure 4.2 PMCA2 expression is not affected by auditory activity.**
Normalized raw intensity (total PMCA2) or average integrated intensity (PMCA2 density) was averaged for all subjects. Each intensity was normalized to the average wildtype raw intensity or average integrated intensity for the controls in that group. There was about a 40% decrease in normalized raw intensity (control=1, *+/dfw*$^{2}$=0.626, deaf=1.086) and normalized average intensity (control=1, *+/dfw*$^{2}$=0.627, deaf=1.093) for *+/dfw*$^{2J}$ as compared to controls. Controls and deaf mice were significantly different from *+/dfw*$^{2J}$ but not from each other (One-way ANOVA; *p≤0.01, N=12, 7, and 6 for Controls, *+/dfw*$^{2J}$, and deaf mice respectively) (error bars=SEM)

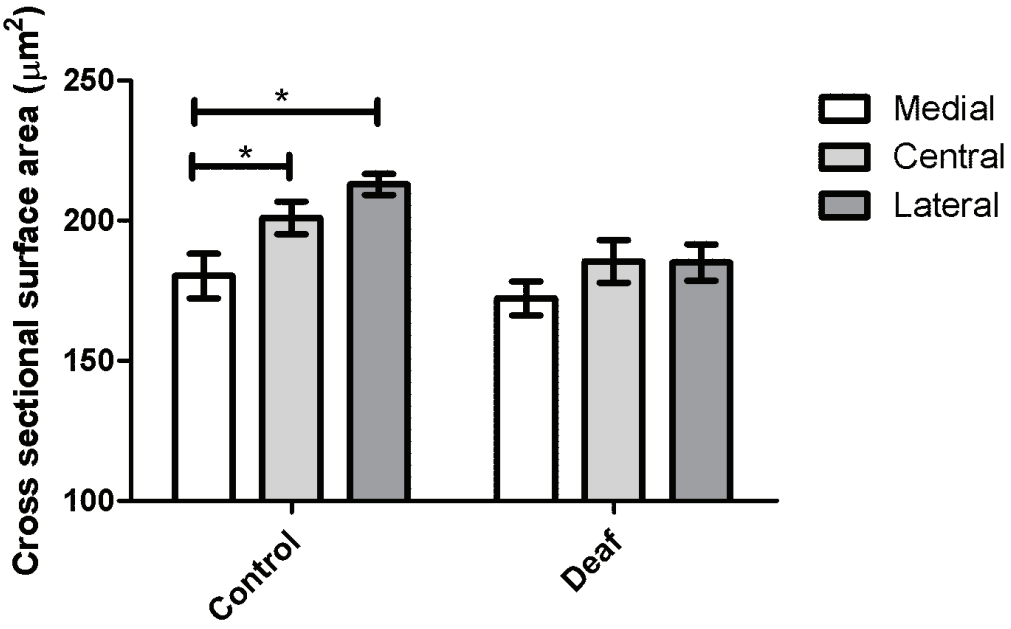


**Figure 4.3 There is a cell size gradient in controls that is absent in deaf mice**. A cell size gradient exists in control mice but is absent in deaf mice. Neuron cross sectional surface area increases medially to laterally in control mice while neuron size is homogenous in deaf mice. (One-way ANOVA; *p≤0.01; N=6 MNTB per condition)

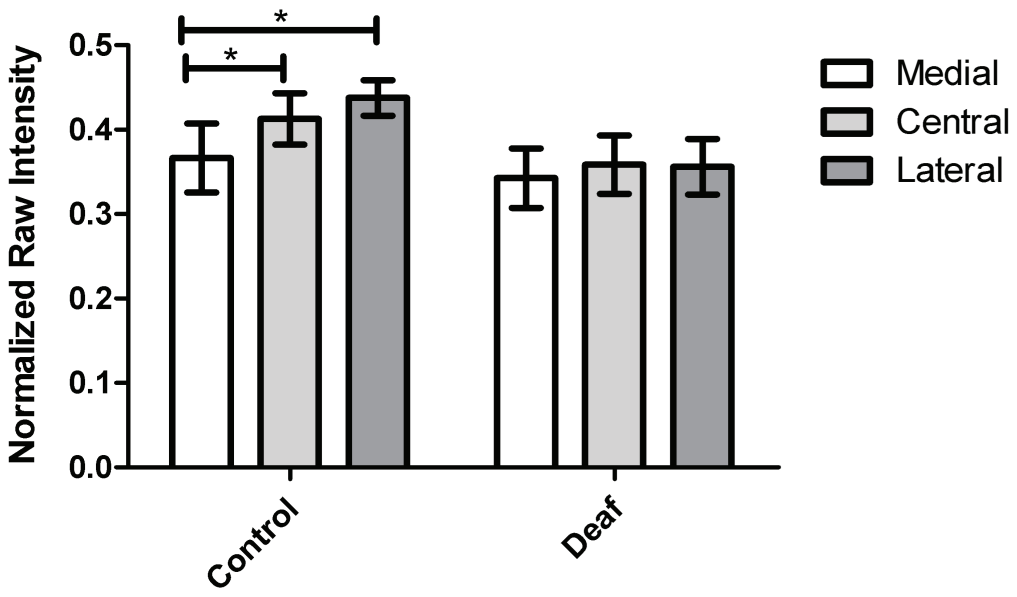


**Figure 4.4 There is a gradient of total PMCA2 in control mice that is absent in deaf mice**

Normalized raw intensity increases medial to laterally in control mice but is homogenous in deaf mice. (One-way ANOVA and Tukey post-hoc analysis; *p≤0.01; N=6 MNTB per condition; Error bars=SEM)

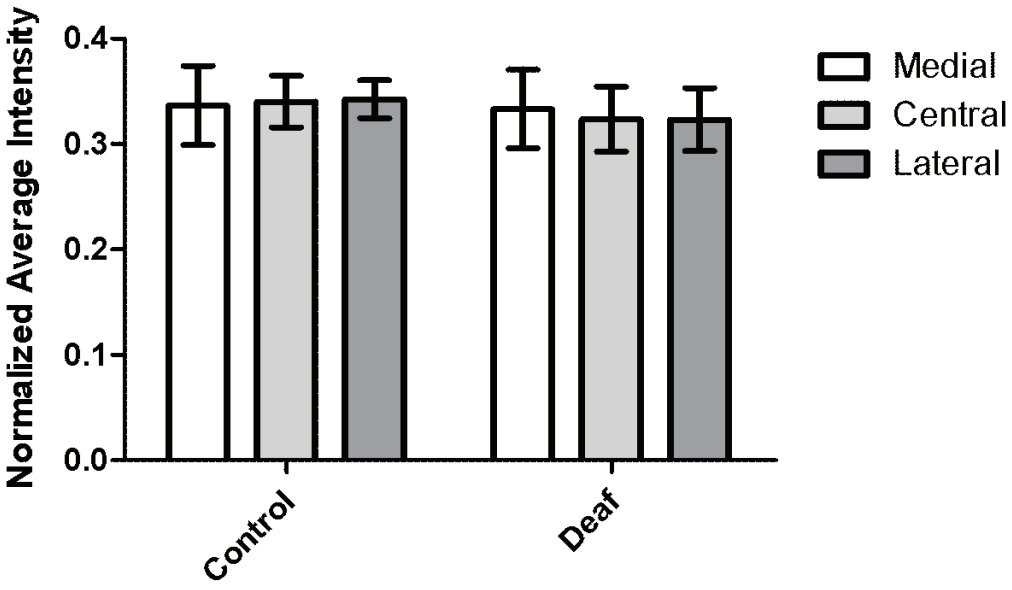


**Figure 4.5 PMCA2 density is homogenously expressed along the tonotopic axis in hearing and deaf mice.** Average intensity is homogenous throughout the MNTB in both control and deaf mice. This suggests that PMCA2 density is similar in control and deaf mice. (One-way ANOVA; N=6 MNTB per condition; Error bars=SEM)

# Chapter 5

## Conclusions

In this thesis we investigate plasma membrane calcium ATPase 2 (PCMA2) localization in the auditory brainstem nuclei focusing on the medial nucleus of the trapezoid body (MNTB). This investigation uncovers a cell size gradient in the MNTB that requires auditory activity. The presence of PMCA2 in the cochlear nucleus (CN), MNTB, and lateral superior olive (LSO) suggests that it is involved in regulating calcium concentrations in these nuclei. At the synaptic level we have evidence that PMCA2 is expressed both pre-synaptically and post-synaptically in the MNTB. This suggests that PMCA2 may be important in maintaining the high firing rate and precision of MNTB neurons.

One mechanism by which PMCA2 might help maintain high firing rates is by pumping calcium in to the synaptic cleft to maintain a high extracellular calcium concentration in order for calcium to enter through voltage gated calcium channels (VGCC) during each depolarization. In addition, PMCA2's calcium clearance may help to maintain fast firing rates by removing calcium to relieve inhibition of VGCC. Both of these mechanisms would help to quickly reset the neuron so it is prepared for the next action potential and allow MNTB neurons to fire quickly. PMCA2 may also play a role in allowing MNTB neurons to be extremely precise by

decreasing facilitation. Pre-synaptic PMCA2 could prevent facilitation by removing the calcium available to induce vesicle release through calcium regulated exocytosis. Post-synaptic PMCA2 may prevent facilitation by decreasing the amount of calcium that is present in the principal cell and maintaining the appropriate calcium concentration in the synaptic cleft so that it takes the same amount of calcium entering through α-amino-3-hydroxy-5-methyl-4-isoxazolepropionic acid (AMPA) receptors to trigger an action potential each time the pre-synaptic cell releases glutamate into the synapse.

While PMCA2 expression is required for hair cell survival it does not appear to be required for MNTB neuron survival at a gross anatomical level. This finding will allow researchers in the future to use PMCA2 mutants to study PMCA2 function with the knowledge that MNTB morphology is unchanged between mutants and controls.

While examining the MNTB of PMCA2 mutants, we discovered a cell size gradient in the MNTB that requires auditory activity. The reason for this cell size gradient is unclear but our capacitance data suggest there is either a functional role or consequence to the variation in cell size. One explanation would be that the differing sizes are a result of differing firing rates. Another explanation may be that these changes in cell size serve as a way for cells to calibrate firing rates by adjusting capacitance. Our data show that not only is auditory activity required to maintain the gradient, but that the gradient returns after a period of deprivation indicating that changes in cell size are plastic. It is possible that MNTB neurons change size in response to inputs to precisely time how fast the post synaptic cell depolarizes. Medial cells fire faster than lateral cells and may decrease cell surface area to decrease capacitance therefore decreasing the time it takes to depolarize the cell. This could be a way for the neurons to maintain temporal

precision. While the discovery of a cell size gradient in the MNTB is fascinating, our findings do not suggest a mechanism for how this gradient comes about or why it exists. This opens a wide area of research that can be done to answer questions about the function of the cell size gradient in the MNTB.

While a gradient in cell size in the MNTB was a novel finding, previous studies have shown ion channels are expressed in gradients along the tonotopic axis. These studies, however, do not take into account the cell size gradient we have discovered. Because cell size increases medial to laterally, if cell size is not controlled for, it may appear there is a medial to lateral ion channel gradient when ion channel density is actually homogenous throughout the MNTB. The cell size gradient may account for previously reported gradients in Kv1.1 and Kv1.3 while gradients in Kv 3.1 and HCN4 may be even more drastic than previously reported (Figure 1.2).

Our study on PMCA2 shows total PMCA2 increases medial to laterally along the tonotopic axis while PMCA2 density is homogenous. This raises interesting questions as to how total PMCA2 and PMCA2 density may have functional effects on MNTB firing. When examining PMCA2 function at the synaptic level it would make sense that PMCA2 density may be more important than total PMCA2. If calcium concentrations at the microdomain level are responsible for the release of neurotransmitter, the concentration of PMCA2 near the active site would be the only relevant PMCA2 in understanding synaptic function. While PMCA2 across the cell may affect calcium concentration of the cytoplasm in general and speed up calcium diffusion away from the active site, our hypothesis is that fast calcium clearance is required at active sites. We hypothesize local PMCA2 is the most important PMCA2 contributing to calcium clearance in the micro domain near the active site. In this way, PMCA2 density may be

the most relevant measurement when attempting to understand PMCA2 function in the MNTB. Since there is no gradient in PMCA2 density in the MNTB, our data suggest that PMCA2 functions similarly in medial and lateral neurons.

This study examined the localization of an important regulator of calcium in hopes that future researchers will be able to use these findings as a guide to design studies that will elucidate what role PMCA2 plays in these neurons. These experiments unexpectedly uncovered a cell size gradient in the MNTB that requires auditory activity. This finding will be important in future studies that attempt to characterize MNTB function and may change the way we look at past studies that did not control for variation in cell size or capacitance. This finding raises many questions as to why auditory activity is required to maintain the cell size gradient, what function the variation in cell size might play, and how these changes in cell size occur. Lastly, we find that PMCA2 is homogenously expressed throughout the MNTB and auditory activity does not affect its expression. Much more work must be done in the future in order to understand the role of PMCA2 in MNTB neurons.

## Bibliography


Antalffy G, Maurer AS, Paszty K, Hegedus L, Padanyi R, Enyedi A, Strehler EE (2012) Plasma membrane calcium pump (PMCA) isoform 4 is targeted to the apical membrane by the w-splice insert from PMCA2. Cell calcium 51:171-178.

Born DE, Rubel EW (1988) Afferent influences on brain stem nuclei of the chicken: presynaptic action potentials regulate protein synthesis in nucleus magnocellularis neurons J Neuroscience 8: 901-919

Bortolozzi M, Brini M, Parkinson N, Crispino G, Scimemi P, De Siati RD, Di Leva F, Parker A, Ortolano S, Arslan E, Brwown SD, Carafoli E, Mammano F (2010) The novel PMCA2 pump mutation Tommy impairs cytosolic calcium clearance in hair cells and links to deafness in mice. The Journal of biological chemistry 285:37693-37703.

Brini M, Coletto L, Pierobon N, Kraev N, Guerini D, Carafoli E. (2003) A comparative functional analysis of plasma membrane Ca2+ pump isoforms in intact cells. The Journal of biologial chemsistry 278:24500-24508.

Brini M, Di Leva F, Domi T, Fedrizzi L, Lim D, Carafoli E (2007) Plasma-membrane calcium pumps and hereditary deafness. Biochem Soc trans 25:913-918.

Carafoli E and Stauffer T. (1994) The plasma membrane calcium pump: functional domains, regulation of the activity, and tissue specificity of isoform expression. J Neurobiol 25; 312-324.

Caride AJ, Filoteo AG, Penniston JT, Strehler EE (2007) The plasma membrane Ca2+ pump isoform 4a differs from isoform 4b in the mechanism of calmodulin binding and activation kinetics: implicaions for Ca2_signaling. J Biol Chem 282:25640-25648.

Doughty JM, Barnes-Davies M, Rusznak Z, Harasztosi C, Forsythe ID (1998) Contrasting Ca2+ channel subtypes at cell bodies and synaptic terminals of rat anterioventral cochlear busy neurons. J Physiol 512:365-376.

Dumont RA, Lins U, Filoteo AG, Penniston JT, Kachar B, Gillespie PG (2001) Plasmamembrane Ca2+-ATPase isoform 2a is the PMCA of hair bundles. J Neurosci *2:*, 5066-5078.

Felmy F, Neher E, Schneggenburger R (2003) Probing the intracellular calcium sensitivity of transmitter release during synaptic facilitation. Cell 37 (5): 801-811.

Ficarella R, Di Leva F, Bortolozzi M, Ortolano S, Donaudy F, Petrillo M, Melchionda S, Lelli A, Domi T, Fedrizzi L (2007) A functional study of plasma-membrane calciumpump isoform 2 mutants causing digenic deafness. Proc Natl Acad Sci U S A 104: 1516-1521.

Forsythe ID (1994) Direct patch recording from identified presynaptic terminals mediating glutamatergic EPSCs in the rat CNS, in vitro. Journal of Physiology 479 (3): 381-387.

Furuta, H, Lin, L, Helper, K, Ryan, A (1998). Evidence for differential regulation of calcium by outer versus inner hair cells: plasma membrane Ca-ATPase gene expression. Hear Res 123, 10-26.

Gazula, VR, Strumbos JG, Mei, X, Chen, H, Rahner, C, Kaczmarek, LK. (2010) Localization of Kv1.3 channels in presynaptic terminals of brainstem auditory neurons. J Comp Neurol 518 (16);3205-3220.

Golub JS, Tong L, Ngyuen TB, Hume CR, Palmiter RD, Rubel EW, Stone JS(2012) Hair cell replacement in adult mouse utricles after targeted ablation of hair cells with diphtheria toxin. J Neurosci 32:15093–15105.

Grothe B, Park TJ (1995) Time can be traded for intensity in the lower auditory system. Naturwissenschaften 82:521-523

Heim R, Hug M, Iwata T, Strehler EE, Carafoli E (1992) Microdiversity of human-plasma-membrane calcium-pump isoform 2 generated by alternative RNA splicing in the N-terminal coding region. European journal of biochemistry 205:333-340.

Hilfiker H, Guerini D, Carafoli E (1994) Cloning and expression of isoform 2 of the human plasma membrane ca2+ ATPase. Funcional properties of the enzyme and its splicing products. J Biol Chem. 269: 26178-26183.

Hill JK, Williams DE, LeMasurier M, Dumont RA, Strehler EE, Gillespie PG. (2006) Splice-site A choice targets plasma-membrane Ca2+-ATPase isoform 2 to hair bundles. J Neuroscience 26:6172-6180.

Hill, JA, Kopp-Scheinpflug, C, Wang, Y, Forsythe, ID, Rubel, EW, and Tempel, BL (2011) *Deafwaddler* Mutants Reveal a Cell Size Gradient in the MNTB. Midwinter Research Meeting of the Association for Research in Otolarangology, Baltimore, MD.

Irvine DR, Parke VN, MccCormikc L (2001) Mechanisms underlying the sensitivity of neurons in the lateral superior olive to interaural intensity differences. J Neurophysiol 86:2647-2666.

Jeffress, LA (1948) A place theory of sound localization. J. Comp. Physiol. Psychol. 41, 35–39

Keeton TP, Burk SE, Shull GE. (1993) Alternative splicing of exons encoding the calmodulin-binding domains and C termini of plasma membrane Ca(2+)-ATPase isoforms 1,2,3 and 4. The Journal of biological chemistry, 268:2740-2748.

Konrad-Martin D, Norton SJ, Mascher KE, Tempel BL (2001) Effects of PMCA2 mutation on DPOAE amplitudes and latencies in deafwaddler mice. Hearing Res, 151, pp 205–220.

Kopp-Scheinpflug C, Dehmel S, Tolnai S, Dietz B, Milenkovic I, Rubsamen R (2008) Glycine-mediated changes of onset reliability at a mammalian central synapse. Neuroscience 157(2):432-445.

Kopp-Scheinpflug C, Fuchs K, Lippe WR, Tempel BL, Rubsamen R (2003) Decreased Temporal Precision of Auditory Signaling in Kcna1-Null Mice: An Electrophysiological Study *In Vivo.* J Neuroscience 23(27): 9199-9207.

Kopp-Scheinpflug C, Steinert JR, Forsythe ID (2011) Modulation and control of synaptic transmission across the MNTB. Hear Res 279:22-31.

Kozel PJ, Davis RR, Krieg EF, Shull GE, Erway LC (2002) Deficiency in plasma membrane calcium ATPase isoform 2 increases susceptibility to noise-induced hearing loss in mice. Hear Res *164*:231-239.

Kozel PJ, Friedman RA, Erway LC, Yamoah EN, Liu LH, Riddle T, Duffy JJ, Doetschman,T, Miller ML, Cardell EL, Shull GE (1998) Balance and hearing deficits in mice with a null mutation in the gene encoding plasma membrane Ca2+-ATPase isoform 2 J. Biol Chem *273*: 18693-18696.

Leao, RN, Sun, H, Svahn, K, Berntson, Youssoufian, M, Paolini, AG, Fyffe, REW, Walmsley, B (2005) Topographic organization in the auditory brainstem of juvenile mice is disrupted in congenital deafness. JPhysiol 571:563-578.

Li, W, Kaczmarek, LK, Perney, TM (2001) Localization of two high –threshold potassium channel subunits in the rat central auditory system. J Comp Neurol 437:196-218.

McCullough BJ, Tempel BL (2004) Haplo-insufficiency revealed in deafwaddler mice when tested for hearing loss and ataxia. Hear Res 195,: 90-102.

Mikaelian D, Ruben RJ (1965): Development of hearing in the normal CBA-J mouse. Acta Otolaryngol (Stockh) 59,451-461.

Moore, MJ, Caspary, DM (1983) Strychnine blocks binaural inhibition in lateral superior olivary neurons. J Neuroscience 3:237-242.

Norton SJ, Tempel BL, Steel KP, Rubel EW (1996) Physiological and anatomical status of the deafwaddler (*dfw*) mutant mouse cochlea. Midwinter Meeting of the Association for Research in Otolaryngology, Abstracts 19, p 82.

Pasic, TR. (1991) Cochlear nuclus cell size is regulated by auditory nerve electrical activity. Otolaryngology head and neck surgery, 104(1):6-13.

Pasic TR, Moore DR, Rubel EW. (1994) Effect of altered neuronal activity on cell size in the medial nucleus of the trapezoid body and ventral cochlear nucleus of the gerbil. J of Comp Neurology, 348(1):111-120.

Penheiter AR, Filoteo AG, Croy CL, Penniston JT (2001) Characterization of the deafwaddler mutant of the rat plasma membrane calcium-ATPase 2. Hearing Res, 162, pp 19–28.

Raleigh, L (1907) On our perception of sound direction. Philos Mag 13;214-232.

Renteria RC, Strehler EE, Copenhagen DR, Krizaj D (2005) Ontogeny of plasma membrane Ca2+ ATPase isoforms in the neural retina of the postnatal rat. Visual Neuroscience 22:263-274.

Schultz JM, Yang Y, Caride AJ, Filoteo AG, Penheiter AR, Lagziel A, Morell RJ, Mohiddin SA, Fananapazir L, Madeo AC, Penniston JT, Griffith AJ (2005) Modification of human hearing loss by plasma-membrane calcium pump PMCA2. N Engl J Med 352, 1557-1564.

Schwarz IR (1992) The superior olivary complex and lateral leminscal nuclei. In: *The Mammalian Auditory Pathway: Neuroanatomy* edited by Webster DB Popper AN, and Fay RR. New York: Springer, 1992, 117-167.

Silverstein, RS Tempel BL (2006) Atp2b2, encoding plasma membrane Ca2+-STPase type 2, (PMCA2) exhibits tissue-specific first exon usage in hair cells, neurons ,and mammary glands of mice. Neuroscience 141:245-257.

Sonntag M, Englitz B, Kopp-Scheinpflug C, Rubsamen R, (2009) Early postnatal development of spontaneous and acoustically evoked discharge activity of principal cells of the meidal nucleus of the trapezoid body: An i*n vivo* study in mice. J Neuroscience 29(30):9510-9520.

Spiden SL, Bortolozzi M, Di Leva F, de Angelis MH, Fuchs H, Lim D, Ortolano S, Ingham NJ, Brini M, Carafoli E, Mammano F, Steel KP (2008) The novel mouse mutation Oblivion inactivates the PMCA2 pump and causes progressive hearing loss. PLoS Genet 4(10):e1000238 Epub.

Stahl WL, Eakin TJ, Ownes JW, Breininger JF, Filuk PE, Anderson WR (1992) Plasma membrane Ca2+-ATPase isoforms: distribution of mRNAs in rat brain by in situ hybridization. Brain research. Molecular brain research, 16:223-231

Street VA, McKee-Johnson JW, Fonseca RC, Tempel BL, Noben-Trauth K (1998) Mutations in a plasma membrane Ca2+-ATPase gene cause deafness in deafwaddler mice. Nat Genet 19: 390-394.

Strehler, EE, Strehler-Page MA, Vogel G, Carafoli E. (1989) mRNAs for plasma membrane calcium pump isoforms differeing in their regulatory domain are generated by alternative splicing that involves tow internal donor sites in a single exon. Proceedings of the National Academy of Sciences of the USA 86:6908-6912.

Strumbos, JG, Brown, MR, Kronengold, J, Polley, DB, Kaczmarek, LK (2010) Fragile X mental retardation protein is required for rapid experience-dependent regulation of the potassium channel Kv3.1b. J Neurocience 30(31):10263-71.

Takahashi K, Kitamura K (1999) A point mutation in a plasma membrane Ca(2+)-ATPase gene causes deafness in Wriggle Mouse Sagami. Biochem Biophys Res Commun *261*: 773- 778.

Taschenberger H, von Gersdorff, H (2000) Fine-tuning an auditory synapse for speed and fidelity: developmental changes in presynaptic waveform, EPSC kinetics, and synaptic plasticity. *J. Neurosci.* 20:9162–9173.

Thompson, SP. (1882) On the function of the two ears in the perception of space. Philos Mag 13;406-416.

Tollin DJ, Yin TCT (2005) Interural phase and level differences sensitivity in low-frequency neurons I nthe lateral superior olive. J Neurosci 25:10648-10657.

Tong L, Hume C, Palmiter R, Rubel E (2011) Ablation of Mouse Cohela Hair Cells by Activating the Human Diptheria Toxin Receptor (DTR) Gene Targeted to the Pou4f3 Locus. ARO Abstract #836

Tritsch NX, Rodriquez-Contreras A, Crins TTH, Wang HC, Borst JG, Bergles DE (2010) Calcium action potentials in hair cells pattern auditory neuron activity before hearing onset. Nature Neuroscience 13 (9): 1050-1052.

von Gersdorff H, Borst JG (2002) Short-term plasticity at the calyx of held. Nature Reviews Neuroscience 3: 53-64.

Von Hehn, CAA, Bhattacharjee, A, Kaczmarek, LK. (2004) Loss of Kv3.1 tonotopicity and alterations in cAMP response element-bindng protein signaling in central auditory neurons of hearing impaired mice. J Neuroscience 24(8): 1936-1940.

Watson, C.J. and Tempel, B.L (2013) A new Atp2b2 deafwaddler allele, interacts strongly with Cdh23 and other auditory modifiers. *Hearing Res*. 304:41-48.

West MJ, Slomianka L, Gundersen H (1991) Unbiased stereological estimation of the total number of neurons in the subdivisions of the rat hippocampus using the optical fractionator. Anat Rec Dec;231(4):482-97.

Wood, JD, Muchinsky, SJ, Filoteo, AG, Penniston, JT, Tempel, BL (2004) Low endolymph calcium concentrations in deafwaddler2J mice suggest that PMCA2 contributes to endolymph calcium maintenance. J Assoc Res Otolaryngol 5:99-110.

Woolf NK, Ryan AF (1984) The development of auditory function in the cochlea of the Mongolian gerbil. Hear Res, Mar; 13(3):277-83.

Yamoah EN, Lumpkin EA, Dumont RA, Smith PJS, Hudspeth AJ, Gillespie PG(1998) Plasma membrane Ca2+-ATPase extrudes Ca2+ from hair cell stereocilia. J Neurosci*18*: 610-624.

## Vita

Jessica Hill Weatherstone was raised in Boise, ID and graduated from Boise High School in 2001. She attended Vassar College in Poughkeepsie, NY where she graduated in 2005 with a BA in Neuroscience and Behavior and a correlate in Chemistry. At Vassar College she studied the effects of dopamine on sexual conditioning of Japanese quail with Dr. Kevin Holloway. After college Jessica moved to San Francisco where she studied decision making behavior and smooth pursuit in macaques in the Heinen and Keller Labs at the Smith-Kettlewell Eye Research Institute. She entered the Department of Pharmacology doctoral program at the University of Washington in 2008 and earned a Doctor of Philosophy in 2014.